For Reference

NOT TO BE TAKEN FROM THIS ROOM

Ex libris
universitatis
albertaensis



For Reference

NOT TO BE TAKEN FROM THIS ROOM

The University of Alberta
Printing Department
Edmonton, Alberta

THE UNIVERSITY OF ALBERTA

SELF BALANCING CAPACITANCE BRIDGE

by

© R. ALLEN WINTER

A THESIS

SUBMITTED TO THE FACULTY OF GRADUATE STUDIES

IN PARTIAL FULFILLMENT OF THE REQUIREMENTS FOR THE DEGREE OF

MASTER OF SCIENCE

DEPARTMENT OF ELECTRICAL ENGINEERING

EDMONTON, ALBERTA

SEPTEMBER, 1968

THE UNIVERSITY OF ALBERTA

SELF BALANCING CAPACITANCE BRIDGE

by

© B. ALLEN WINTER

A THESIS

SUBMITTED TO THE FACULTY OF GRADUATE STUDIES

IN PARTIAL FULFILLMENT OF THE REQUIREMENTS FOR THE DEGREE OF

MASTER OF SCIENCE

DEPARTMENT OF ELECTRICAL ENGINEERING

EDMONTON, ALBERTA

SEPTEMBER, 1958

Thesis
1968 (F)
240

UNIVERSITY OF ALBERTA

FACULTY OF GRADUATE STUDIES

The undersigned certify that they have read, and recommend to the Faculty of Graduate Studies for acceptance, a thesis entitled "Self Balancing Capacitance Bridge", submitted by R. Allen Winter in partial fulfillment of the requirements for the degree of Master of Science.

ABSTRACT

This thesis is a feasibility study which describes the design, development, and construction of an instrument to measure capacitors automatically.

Capacitance is measured by adjusting two variable resistors in a Wien bridge until the balance conditions are achieved. Servomotors are used for driving the variable resistors. The bridge can be balanced by adjusting each potentiometer once only, provided the measuring circuits are accurate. The range of measurement is from .001μF to 1.0μF, with the error typically less than 0.1% of the unknown. All of the active circuits constructed utilize silicon semiconductors.

Digitized by the Internet Archive
in 2020 with funding from
University of Alberta Libraries

https://archive.org/details/Winter1968

ACKNOWLEDGMENTS

The author wishes to thank the staff members and graduate students of the Department of Electrical Engineering for their co-operation during the course of this work.

The author particularly wishes to acknowledge his indebtedness for the advice and assistance of Professor Y. J. Kingma, under whose supervision this project was carried out. Also, the author would like to express his appreciation of the continued patience and encouragement given by his parents during the preparation of this thesis.

The financial assistance provided by the National Research Council and the University of Alberta is very gratefully acknowledged by the author.

TABLE OF CONTENTS

		Page
CHAPTER 1:	INTRODUCTION	
1.1	Specifications	1
1.2	Basic Bridge Equations	2
CHAPTER 2:	BRIDGE THEORY	
2.1	Introduction	4
2.2	Locus of $\frac{e_d}{e_s}$ for Variable R_T	4
2.3	Locus of $\frac{e_d}{e_s}$ for Variable R_N	7
2.4	Combined Locus of $\frac{e_d}{e_s}$ (R_T,R_N)	9
2.5	Comparison of Balancing Procedures	10
CHAPTER 3:	BLOCK DIAGRAMS	
3.1	Introduction	12
3.2	System Block Diagram	12
3.3	Circuit Block Diagram	13
CHAPTER 4:	CIRCUIT DESCRIPTIONS	
4.1	Bridge Detector	16
4.2	Automatic Gain Control (A.G.C.)	17
4.3	Phase Detector	20
4.4	Amplifying Circuits for Phase Detector	26
4.5	Additional Circuits for Phase Detector	29
4.6	Magnitude Detector and Amplifying Circuits	33
4.7	Magnitude Detector Polarity Circuits	40
4.8	Sequence of Motor Operation	40
4.9	Servomotor Circuits	44

		Page
CHAPTER 5:	PERFORMANCE OF INSTRUMENT	
5.1	Introduction	46
5.2	Balancing Process	46
5.3	Effects of Noise and Stray Capacitance	47
5.4	Results	49
5.5	Conclusion	51
LIST OF REFERENCES		52
APPENDICES:		
I	Locus of a Circle	53
II	Specifications of μA 709	56
III	Specifications of μA 710	59
IV	Discrete Component Operational Amplifier	61
V	Effect of Stray Capacitances	63
VI	Mechanical Components	65

LIST OF FIGURES

FIGURE	TITLE	PAGE
1.1	Wien Bridge	2
1.2	Equivalent Circuits for Z_S	2
2.1	Locus of Equation 2.5	5
2.2	Locus of $\frac{ed}{es}$ (RT) for Different Values of R_N	7
2.3	Locus of $\frac{ed}{es}$ (RN) for Different Values of R_T	9
2.4	Locus of $\frac{ed}{es}$ (RT, RN) for Fictitious Measurement	10
2.5	Locus of $\frac{ed}{es}$	10
2.6	Manual Balancing Procedure	11
2.7	Balancing Procedure Suggested in Section 2.5	11
3.1	Block Diagram of System	14
3.2	Block Diagram of the Main Circuits	14
4.1	Bridge Detector	16
4.2	A.G.C. Circuit	18
4.3	Phase Detector	23
4.4	Polarity Conversion for Phase Detector	24
4.5	Waveforms in Phase Detector	25
4.6	Amplifiers for Phase Detector	27
4.7	Required Transfer Function	29
4.8	Transfer Function of Figure 4.3	29
4.9	Modified Transfer Function	30
4.10(a)	Additional Circuitry for Proper Transfer Function	31
4.10(b)	Additional Circuitry for Proper Transfer Function	32
4.11	Magnitude Detector and Amplifying Circuits	36
4.12	Magnitude Detector Polarity Circuits	41
4.13	Effect of Small Angular Error	42
4.14	Motor Sequencing Circuits	43

4.15	Motor Control Switch	43
4.16	Motor Amplifiers and 400 Hz Modulator	45
5.1	Wien Bridge Circuit	48
A 2.1	Schematic Diagram of μA 709	57
A 3.1	Schematic Diagram of μA 710	60
A 4.1	Typical Operational Amplifier	62
A 6.1	Diagram of Mechanical Bridge Components	66

(NOTE: In all figures, the resistance values are given in K ohms and the capacitance values in μF, unless otherwise stated.)

LIST OF GRAPHS

GRAPH	TITLE	PAGE
1	Experimental Magnitude and Phase Angle Curves of A_1 and A_2 (Figure 4.2)	21
2	Magnitude Curve of Cascaded Filters (Figure 4.2)	22
3	Experimental Magnitude and Phase Angle Curves of A_1 (Figure 4.6)	28
4	Transfer Function for Phase Detector	34
5	Error in Phase Angle as One Input Changes Amplitude	35
6	Experimental Magnitude Curves of A_1 (Figure 4.11) for Three Input Levels	38
7	Transfer Function of Magnitude Detector	39

CHAPTER 1

INTRODUCTION

There are various automatic capacitance bridges currently on the commercial market. None of these, however, measure the unknown by utilizing positional devices for varying resistance in a bridge circuit. It is the intention of this study to show that a practical and accurate method of automatically measuring capacitors may be accomplished by driving each of the two balancing rheostats in a Wien bridge with a servomotor. Also desired is a balancing procedure having the least number of alternate adjustments to each variable resistor. This is as opposed to the process of balancing a manual impedance bridge where a number of alternate adjustments are required due to the convergent nature of the process.

1.1 SPECIFICATIONS

In the design of the instrument, the following specifications were decided upon:

1. The instrument would make measurements at one frequency ($1KH_z$).
2. Unknown components would be restricted to capacitors.
3. Capacitors would have dissipation factors of less than 1.0 at $1KH_z$.
4. Measurement range would extend over three decades (.001μF to 1.0μF).
5. Accuracy of the capacitance would be better than 0.5%.
6. Range selection would be manual.
7. The balancing components would be variable resistors driven by 400 H_z servomotors.

These specifications do not describe an automatic instrument but, rather, an instrument which measures automatically once the proper conditions for measurement have been met. The reason for this approach arises from

the fact that this study is primarily concerned with demonstrating the accuracy and practicality of this type of instrument; and not for the purpose of contributing to the already comprehensive bridge theory now published. The complete automation of the instrument (i.e. selection of the proper bridge configuration and components suitable for measuring the unknown's magnitude and losses) could come at a later date without affecting the balancing procedure and accuracy.

1.2 BASIC BRIDGE EQUATIONS

The circuit used for measuring capacitance is the Wien bridge (figure 1.1) where the unknown (Zs) forms one arm of the bridge.

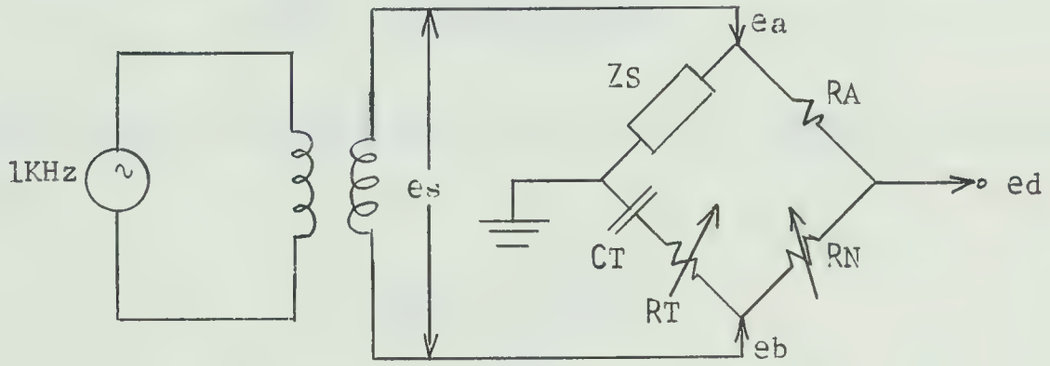


Figure 1.1 Wien Bridge

The unknown lossy capacitor may be represented by two equivalent circuits (figures 1.2(b) and 1.2(c)).

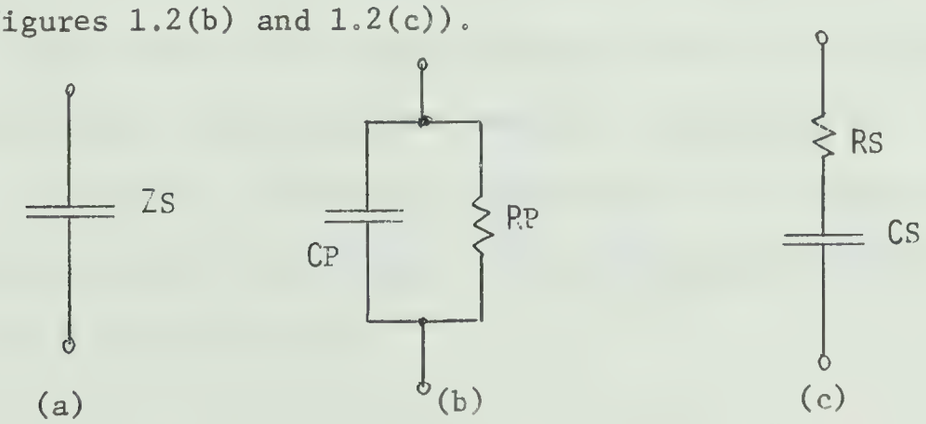


Figure 1.2 Equivalent Circuits for Zs

The relationships[7] between these circuits are given by equations 1.1 to 1.4.

$$Rs = \frac{D^2}{1+D^2} Rp \qquad (1.1) \qquad Rp = \left(\frac{D^2+1}{D^2}\right) Rs \qquad (1.3)$$

$$Cs = (D^2+1)Cp \qquad (1.2) \qquad Cp = \left(\frac{1}{1+D^2}\right) Cs \qquad (1.4)$$

$$\left(\text{where } D = \frac{1}{\omega CpRp} = \omega CsRs\right).$$

For convenience of analysis, the unknown will be considered as the series equivalent circuit (figure 1.2(c)). Values for the parallel circuit are readily calculated from the equations.

The bridge output (ed) is given by equation 1.5[9].

$$\frac{ed}{es} = \frac{RNZS - RAZT}{(RA+RN)(ZS+ZT)} \qquad (1.5)$$

The equations giving the conditions for balance are easily derived from equation 1.5:

$$RS = \left(\frac{RA}{RN}\right) RT = \left(\frac{CT}{CS}\right) RT \qquad (1.6)$$

$$CS = \left(\frac{RN}{RA}\right) CT \qquad (1.7)$$

To determine the optimum operating sequence of the rheostats RT and RN to obtain a null requires analysis of equation 1.5. This is done in Chapter 2 where it is shown that adjustment of each rheostat once only is all that is required for balance. The corresponding conditions and requirements are also derived.

CHAPTER 2

BRIDGE THEORY

2.1 INTRODUCTION

In order to determine the optimum operating sequence of the balancing process, it is necessary to determine how $\frac{ed}{es}$ is affected as each of the variables changes. This must be done in the complex plane since there is an angle and a magnitude associated with $\frac{ed}{es}$ for all values of each parameter. Since all parameters in equation 1.5 are constant except for RT and RN once balancing has started, only the loci for these two parameters will be investigated.

2.2 LOCUS OF $\frac{ed}{es}$ FOR VARIABLE RT

The locus of $\frac{ed}{es}$ for varying RT will be studied first. Substituting the terms for ZT and ZS into equation 1.5 results in:

$$Z_T = R_T + \frac{1}{j\omega C_T} \tag{2.1}$$

$$Z_S = R_S + \frac{1}{j\omega C_S} \tag{2.2}$$

$$\frac{ed}{es} = \left(\frac{1}{R_A + R_N}\right) \frac{(R_N R_S - R_A R_T) - j\frac{1}{\omega}\left(\frac{R_N}{C_S} - \frac{R_A}{C_T}\right)}{(R_S + R_T) - j\frac{1}{\omega}\left(\frac{1}{C_S} + \frac{1}{C_T}\right)} \tag{2.3}$$

Rearranging the terms in equation 2.3 yields equation 2.4.

$$\frac{ed}{es}(R_T) = \left(\frac{1}{R_A + R_N}\right) \frac{\left[\frac{1}{\omega}\left(\frac{R_N}{C_S} - \frac{R_A}{C_T}\right) + jR_N R_S\right] + j(-R_A) R_T}{\left[\frac{1}{\omega}\left(\frac{1}{C_S} + \frac{1}{C_T}\right) + jR_S\right] + J R_T} \tag{2.4}$$

Equation 2.4 may be put in the form of equation 2.5.

$$f(x) = \frac{a + jbx}{c + jx} = b + \frac{a - bc}{c + jx} \tag{2.5}$$

a, b, c are complex constants

x is the variable

It is shown in Appendix I that equation 2.5 represents a circle in the complex plane for varying X. The radius and co-ordinates of the center of the circle are given by:

$$\text{Radius} = \frac{|a - bc|}{2\ \text{Re}\{c\}} \tag{2.6}$$

Center {Uc,Vc}:

$$Uc = \text{Re}\{b\} + \frac{\text{Re}\{a - bc\}}{2\ \text{Re}\{c\}} \tag{2.7}$$

$$Vc = \text{Im}\{b\} + \frac{\text{Im}\{a - bc\}}{2\ \text{Re}\{c\}} \tag{2.8}$$

The locus of equation 2.5 in the complex plane for all values of X is illustrated in figure 2.1.

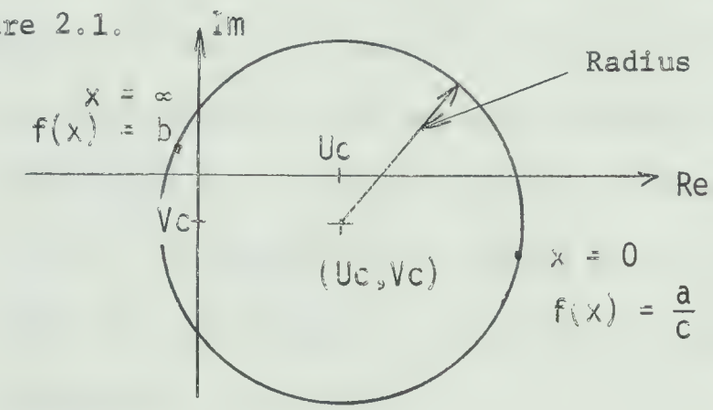


Figure 2.1 Locus of Equation 2.5

Due to the similarities between equations 2.4 and 2.5 (where the variable X is now RT, and the constant a, b, and c are related to the other bridge components), it is evident that the locus of equation 2.5 is a circle. After substituting the appropriate terms for 'a', 'b', and 'c', and simplifying, the radius and center are obtained.

$$Uc = -\frac{RA}{RA + RN} + \frac{CT}{2\ (Cs + Cr)} \tag{2.9}$$

$$Vc = \frac{Rs}{\frac{2}{\omega}\left(\frac{1}{CT} + \frac{1}{Cs}\right)} \tag{2.10}$$

$$\text{Radius} = \frac{|Zs|}{\frac{2}{\omega}\left(\frac{1}{CT} + \frac{1}{Cs}\right)} \tag{2.11}$$

Also of interest are the endpoints of the semicircle (only positive values of the variable RT are possible).

$$\frac{ed}{es}(RT)\Big|_{RT=\infty} = -\frac{RA}{RA + RN} \tag{2.12}$$

$$\frac{ed}{es}(RT)\Big|_{RT=0} = \frac{RNRS + \frac{1}{j\omega}\left(\frac{RN}{CS} - \frac{RA}{CT}\right)}{(RA + RN)\left[RS + \frac{1}{j\omega}\left(\frac{1}{CS} + \frac{1}{CT}\right)\right]} \tag{2.13}$$

$$= -\frac{RA}{RA + RN} + \frac{RS + \frac{1}{j\omega CS}}{RS + \frac{1}{j\omega}\left(\frac{1}{CS} + \frac{1}{CT}\right)} \tag{2.14}$$

From equations 2.9 to 2.14, the following characteristics about the circle are evident (for specific unknown and reference components):

1. The locus is a semicircle and travels clockwise as RT increases.
2. One end point ($RT = \infty$) is always on the negative real axis.
3. The other end point ($RT = 0$) always has a positive imaginary component.
4. The radius is independent of RA and RN.
5. The imaginary coordinate for the center is positive and independent of RA and RN.
6. The imaginary coordinate for the two endpoints are positive and independent of RA and RN.
7. The real components of the end points and the center become more positive (or less negative) as RN increases.

The information from the preceding seven points reveals that the size and orientation of the circle are independent of RN, and that increasing RN only shifts the circle horizontally to the right. Figure 2.2 illustrates the locus of $\frac{ed}{es}$ (RT) for certain values of RN.

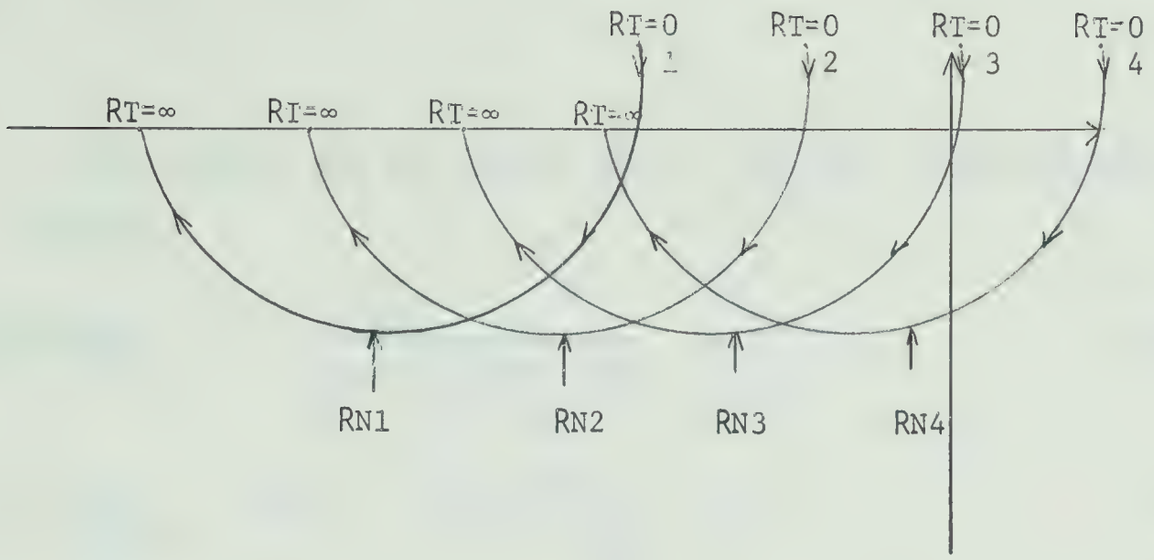


Figure 2.2 Locus of $\frac{ed}{es}$ (RT) for Different Values of RN

Referring to the figure, each of the curves (1, 2, 3, and 4) represent the locus of $\frac{ed}{es}$ (RT) for one value of RN (RN1, RN2, RN3, and RN4) as RT varies from zero to infinity.

2.3 LOCUS OF $\frac{ed}{es}$ FOR VARIABLE RN

The locus of $\frac{ed}{es}$ (RN) is obtained by a similar procedure as for $\frac{ed}{es}$ (RT). The following equation results:

$$\frac{ed}{es}(RN) = \frac{j\left[\dfrac{-RART + j\frac{RA}{\omega CT}}{(RS + RT) - j\frac{1}{\omega}\left(\frac{1}{CS} + \frac{1}{CT}\right)}\right] + j\left[\dfrac{RS - j\frac{1}{\omega CS}}{(RS + RT) - j\frac{1}{\omega}\left(\frac{1}{CS} + \frac{1}{CT}\right)}\right] RN}{(jRA) + j\,RN} \qquad (2.15)$$

This is simplified with the aid of equation 2.5.

$$\frac{ed}{es}(RN) = \frac{ZS}{ZS + ZT} - \frac{RA}{RA + RN} \qquad (2.16)$$

$$= b - \frac{RA}{RA + RN} \qquad (2.17)$$

The locus is not a circle, but a straight horizontal line, which travels from left to right as RN increases. The value of 'b' is one end point (RN = ∞) of the locus and establishes the location of the line in the polar plane. For a given situation, then, the position of $\frac{ed}{es}$ on the straight line depends upon RN and the location of the line depends on 'b' and hence RT.

The locus of the end points (RN = ∞ and RN = 0) can be shown to be circles.

$$\frac{ed}{es}(RN)\Big|_{RN=\infty} = b = \frac{j\ Zs}{(jZs + \frac{1}{\omega CT}) + jRT} \tag{2.18}$$

$$\frac{ed}{es}(RN)\Big|_{RN=0} = b - 1 = \frac{jZs}{(jZs + \frac{1}{\omega CT}) + jRT} - 1 \tag{2.19}$$

The two circles are identical, but with a horizontal translation. The characteristics of the circle for RN = ∞ are obtained with the aid of equations 2.5 to 2.8.

$$Uc = \frac{CT}{2\ (Cs + CT)} \tag{2.20}$$

$$Vc = \frac{Rs}{\frac{2}{\omega}\ (\frac{1}{CT} + \frac{1}{Cs})} \tag{2.21}$$

$$\text{Radius} = \frac{|Zs1|}{\frac{2}{\omega}\ (\frac{1}{CT} + \frac{1}{Cs})} \tag{2.22}$$

$$b\ (RT)\Big|_{RT=\infty} = 0 \tag{2.23}$$

$$b\ (RT)\Big|_{RT=0} = \frac{Rs + \frac{1}{j\omega Cs}}{Rs + \frac{1}{j\omega}\ (\frac{1}{Cs} + \frac{1}{CT})} \tag{2.24}$$

$$= \frac{Rs^2 + \frac{1}{\omega^2 Cs}\ (\frac{1}{CT} + \frac{1}{Cs}) + j\ \frac{Rs}{\omega CT}}{Rs^2 + \frac{1}{\omega^2}\ (\frac{1}{Cs} + \frac{1}{CT})^2} \tag{2.25}$$

The locus for $\frac{ed}{es}$ (RN) is now easily obtained (figure 2.3).

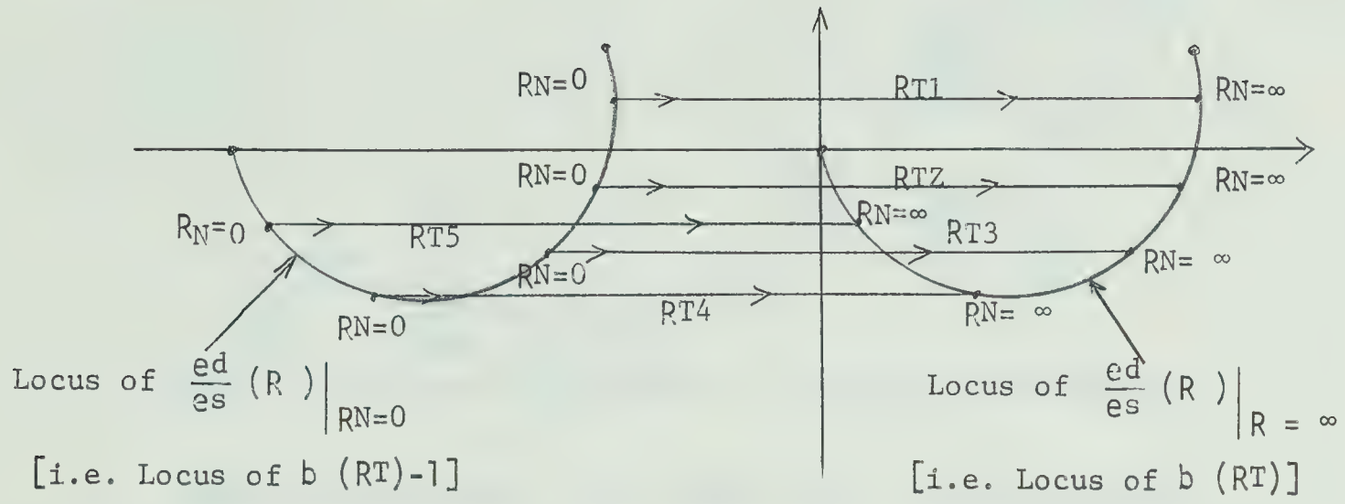


Figure 2.3 Locus of $\frac{ed}{es}$ (RN) for Different Values of RT.

It is apparent from figure 2.3 that once RT has been set to any value and RN is varied, the locus is on a straight horizontal line.

2.4 COMBINED LOCUS OF $\frac{ed}{es}$ (RT,RN)

The information in the preceding two sections may now be used to illustrate the locus of $\frac{ed}{es}$ (RT,RN) during a fictitious measurement. Once the proper reference components for the bridge have been suitably selected for the unknown, all parameters in equation 2.3, except RN and RT, become constant.

Figure 2.4 demonstrates the locus of $\frac{ed}{es}$ as RN and RT are varied one at a time. The fictitious measurement procedure illustrated obviously is not an efficient one, but it does illustrate the previous two sections. The first adjustment is to RN, as RNO changes to RN1 (RT remaining fixed at RTO). This portion of the locus is a straight horizontal line, i.e. the imaginary component remains constant. The second adjustment changes RTO to RT2 (RN remaining fixed at RN1). This part of the locus is an arc and corresponds to one of the curves in figure 2.2. This procedure is continued until $\frac{ed}{es}$ becomes zero.

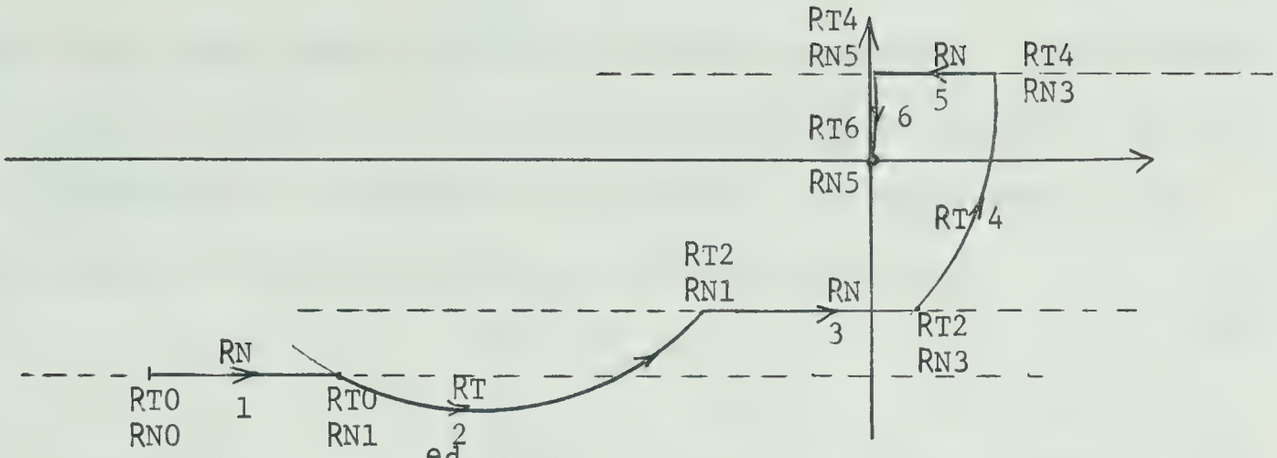


Figure 2.4 Locus of $\frac{ed}{es}$ (RT,RN) for Fictitious Measurement.

From the foregoing, it is obvious that once the imaginary component of $\frac{ed}{es}$ has been made equal to zero, it will remain so as long as only RN is changed. This condition is achieved by adjusting RT until the locus crosses the real axis. Adjusting RN now causes the locus to move along the real axis to the origin (i.e. $\frac{ed}{es} = 0$). This then is a method of balancing a bridge in only two operations for any unknown capacitor. Figure 2.5 shows the balancing procedures for a capacitor.

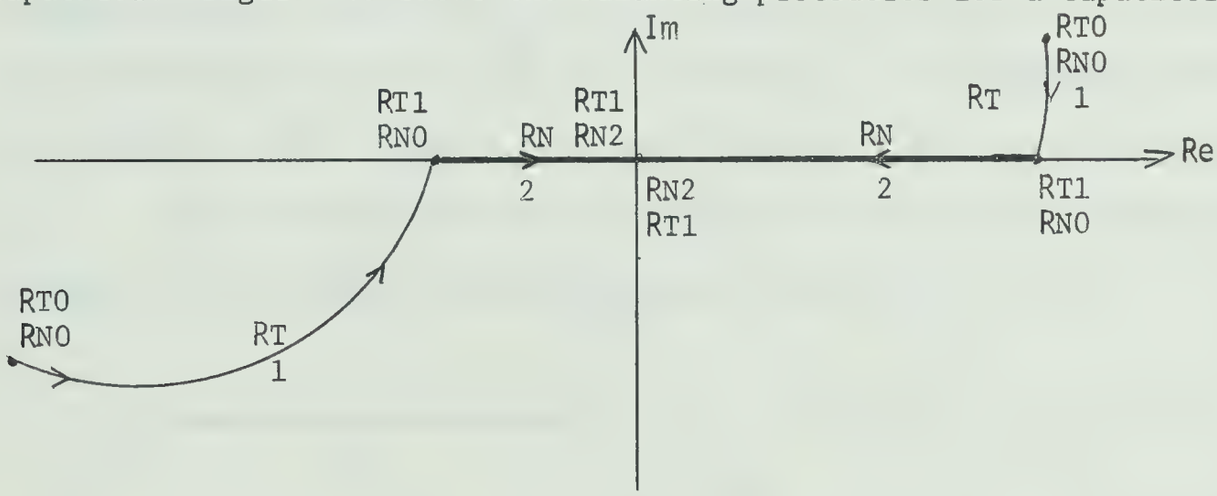
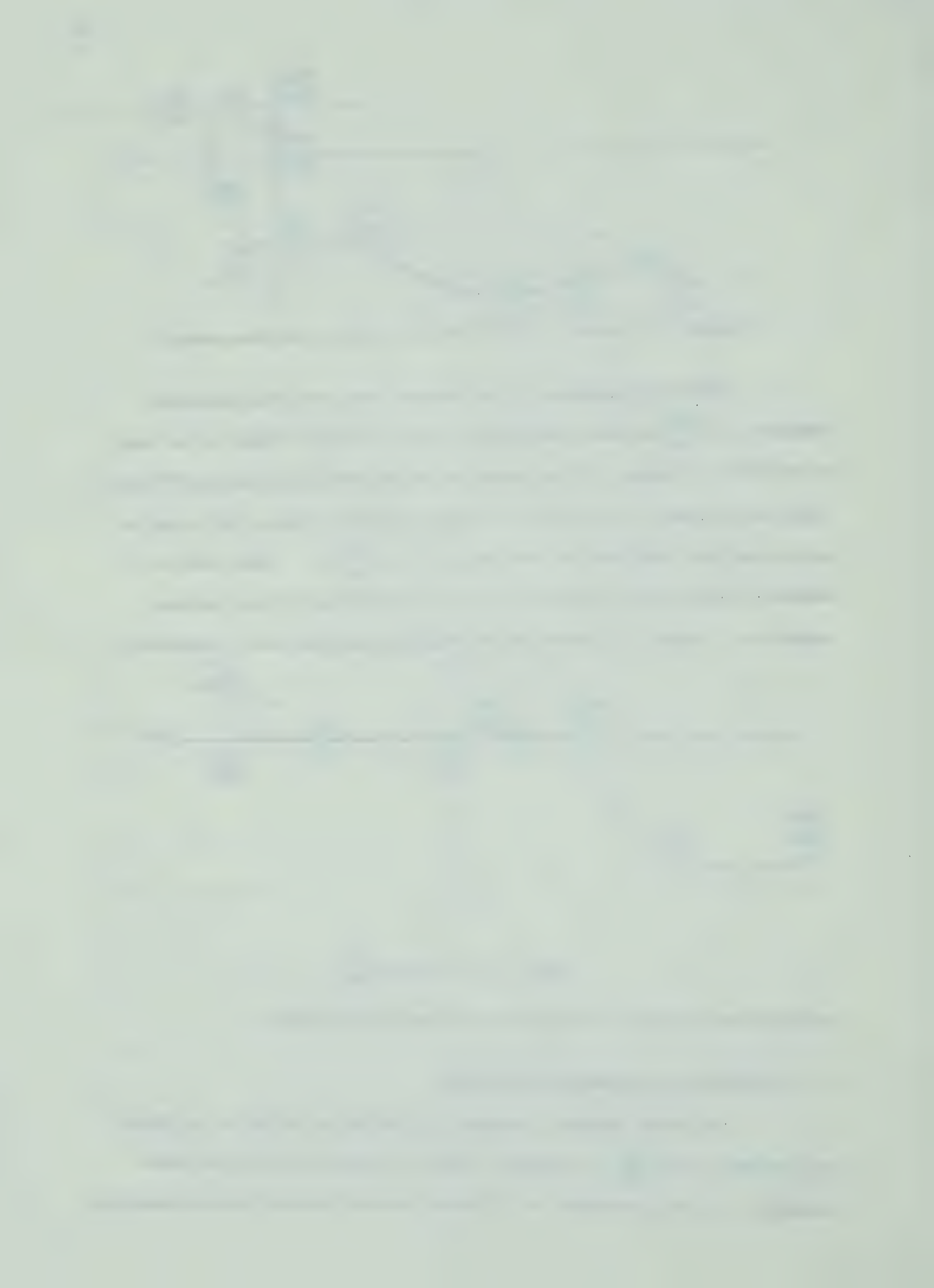


Figure 2.5 Locus of $\frac{ed}{es}$

Two different initial conditions for RT and RN are shown.

2.5 COMPARISON OF BALANCING PROCEDURES

The normal method of manually balancing a bridge is to adjust one variable until $\frac{ed}{es}$ is a minimum, then to repeat this for the other variable. If this procedure is followed, perfect balance is not possible;



however a very small value of $\frac{ed}{es}$ will eventually be reached. This procedure is illustrated in figure 2.6 for a situation where $\frac{ed}{es}$ is small (so that the loci of $\frac{ed}{es}$ (RT) may be approximated by straight lines which are parallel to the tangent of the locus where it crosses the real axis).

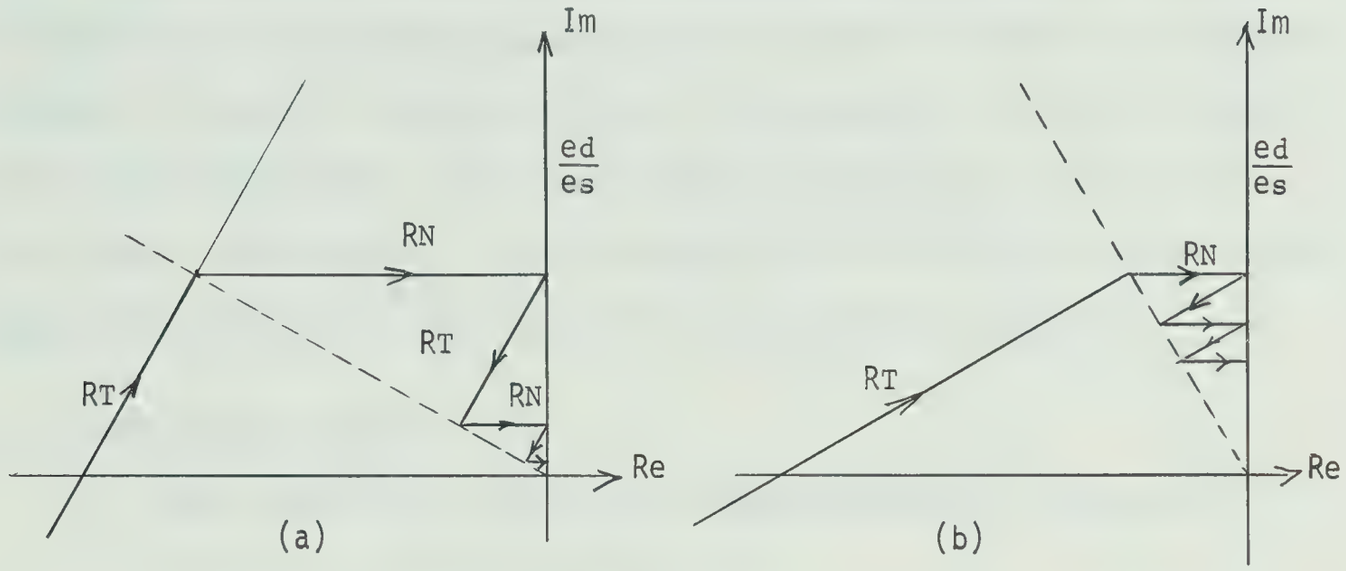


Figure 2.6 Manual Balancing Procedure

Comparing figures 2.6 (a) and 2.6 (b) shows that the balancing procedure is slower when the slope of $\frac{ed}{es}$ (RT) is smaller. This situation corresponds to a capacitor with a higher value of D (a lower value of parallel resistance).

The balancing procedure suggested in Section 2.4 is shown in figure 2.7 for the same situations as used for figure 2.6.

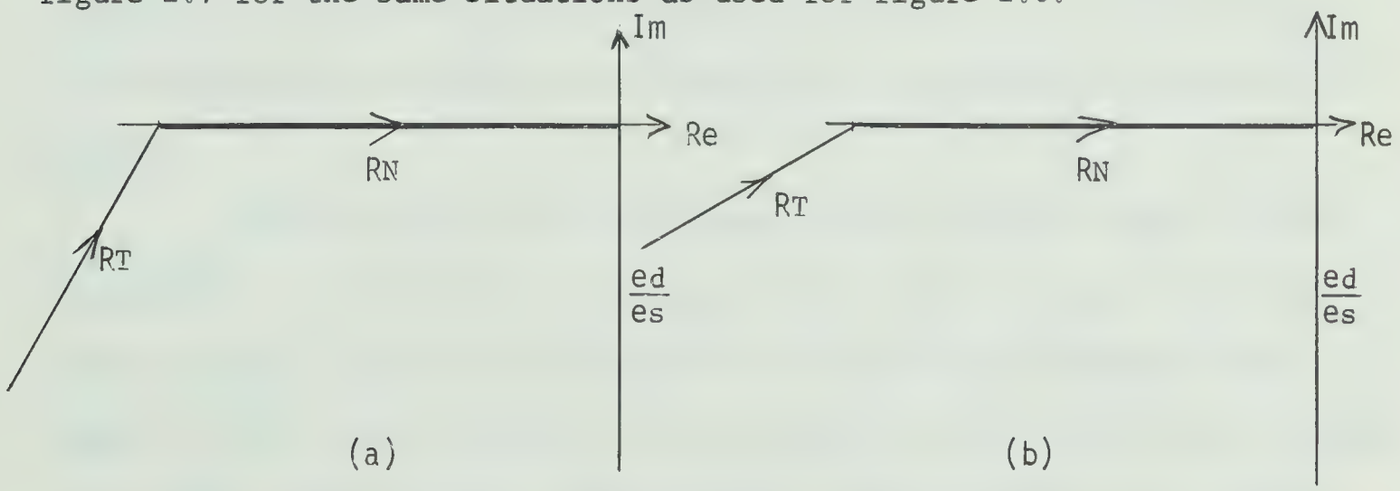


Figure 2.7 Balancing Procedure Suggested in Section 2.5

Obviously, balance is attained much faster using the method suggested in Section 2.4, which is not affected by the slope of $\frac{ed}{es}$ (RT) (i.e. the dissipation (I of the unknown).

CHAPTER 3

BLOCK DIAGRAMS

3.1 INTRODUCTION

To implement the basic scheme of balancing the bridge as suggested in Chapter 2, it is necessary to decide on the general scheme to be employed, and also the type of circuits which will be necessary. The use of a system block diagram simplifies the task of arranging the general circuits in their proper relationship. The realization of the blocks with circuit block diagrams then simplifies the design of the appropriate circuits.

3.2 SYSTEM BLOCK DIAGRAM

The bridge output (ed) must be separated into two components:

1) Phase angle of ed with respect to es
2) Magnitude of ed (and hence $\frac{ed}{es}$)

These become the inputs to the motors, which in turn drive the rheostats. As shown in figure 3.1, phase angle is the input to the motor driving RT, and magnitude is the input to motor RN. The input to the system is the unknown capacitor (CS,RS), and the outputs of the system are RN and RT. The equilibrium values of RN and RT (balance conditions) are simply related to CS and RS through the gain of the bridge (i.e. the reference components RA and CT).

The Wien bridge, when considered alone, has four inputs: CS, RS, RN, and RT. CS and RS would correspond to the variable inputs in a normal control system, while RN and RT would be similar to the feedback signals. Since CS and RS remain constant, the operation of the system shown in figure 3.1 would be like that of a system having a constant input, with certain initial values at time t=0. The values of RN and RT at t=0 would correspond to these initial conditions. The system would begin operation at t=0 in a

manner such that the error signals tend to decrease to zero. When zero is reached, the outputs have reached their equilibrium value and the bridge is balanced.

The normalized output voltage of the bridge is given in equation 2.3, and is repeated again for convenience.

$$\left(\frac{ed}{es}\right) = \left(\frac{1}{RA + RN}\right) \frac{(RNRS - RART) - j\frac{1}{\omega}\left(\frac{RN}{CS} - \frac{RA}{CT}\right)}{(RS + RT) - j\frac{1}{\omega}\left(\frac{1}{CS} + \frac{1}{CT}\right)} \tag{3.1}$$

The expressions for ϕ and $\left|\frac{ed}{es}\right|$ are easily obtained from equation 3.1.

$$\phi = \tan^{-1} \frac{(RA + RN)\left(\frac{RS}{CT} - \frac{RT}{CS}\right)}{\omega\left[(RS + RT)(RNRS - RART) + \frac{1}{\omega^2}\left(\frac{1}{CS} + \frac{1}{CT}\right)\left(\frac{RN}{CS} - \frac{RA}{CT}\right)\right]} \tag{3.2}$$

$$\left|\frac{ed}{es}\right| = \left\{\frac{(RNRS - RART)^2 + \frac{1}{\omega^2}\left(\frac{RN}{CS} - \frac{RA}{CT}\right)^2}{(RA + RN)^2\left[(RS + RT)^2 + \frac{1}{\omega^2}\left(\frac{1}{CT} + \frac{1}{CS}\right)^2\right]}\right\}^{1/2} \tag{3.3}$$

3.3 CIRCUIT BLOCK DIAGRAM

The main circuits required to realize the block diagram of figure 3.1 are shown in figure 3.2. The source for the bridge is obtained from a transformer which is driven by a 1KHz oscillator. This permits one of the bridge output leads to be grounded. This greatly simplifies the design of the bridge detector, since there is no common mode signal when the bridge is balanced.

The bridge detector is a unity gain buffer having very high input impedance, very low output impedance, and no phase shift at 1KHz. The high input impedance is necessary to prevent the locus of $\frac{ed}{es}$ from being rotated and consequently nullifying the theory of Chapter 2. The low output impedance is required in order to drive the following circuits.

The magnitude detector amplifies ed, then rectifies and filters it.

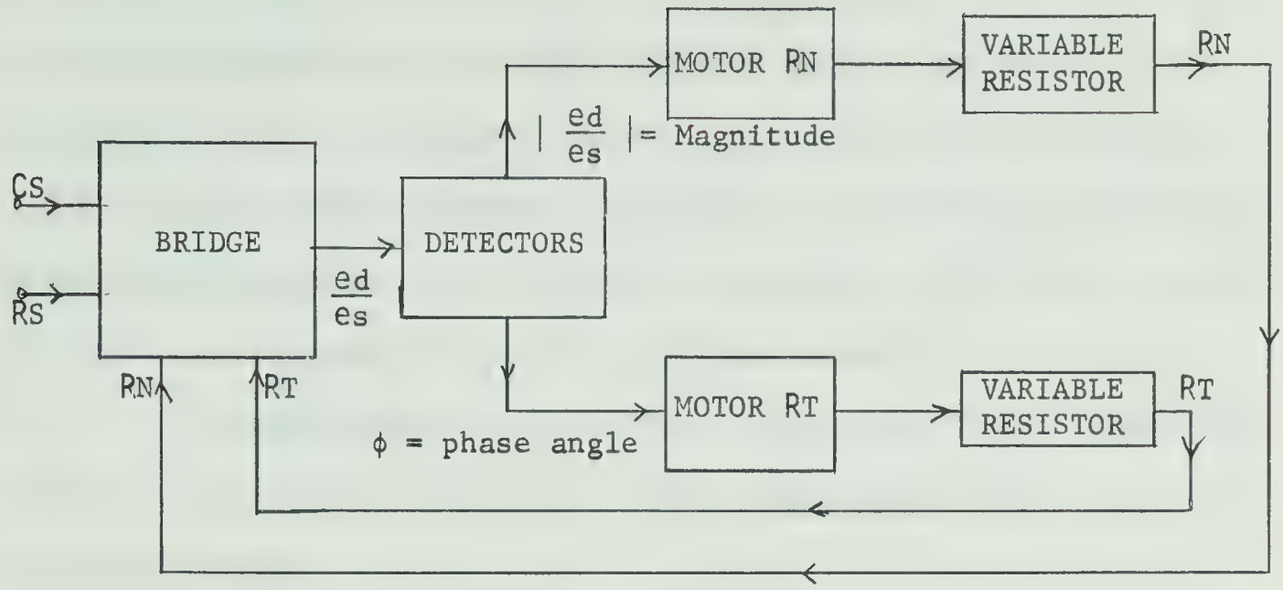


Figure 3.1 Block Diagram of System

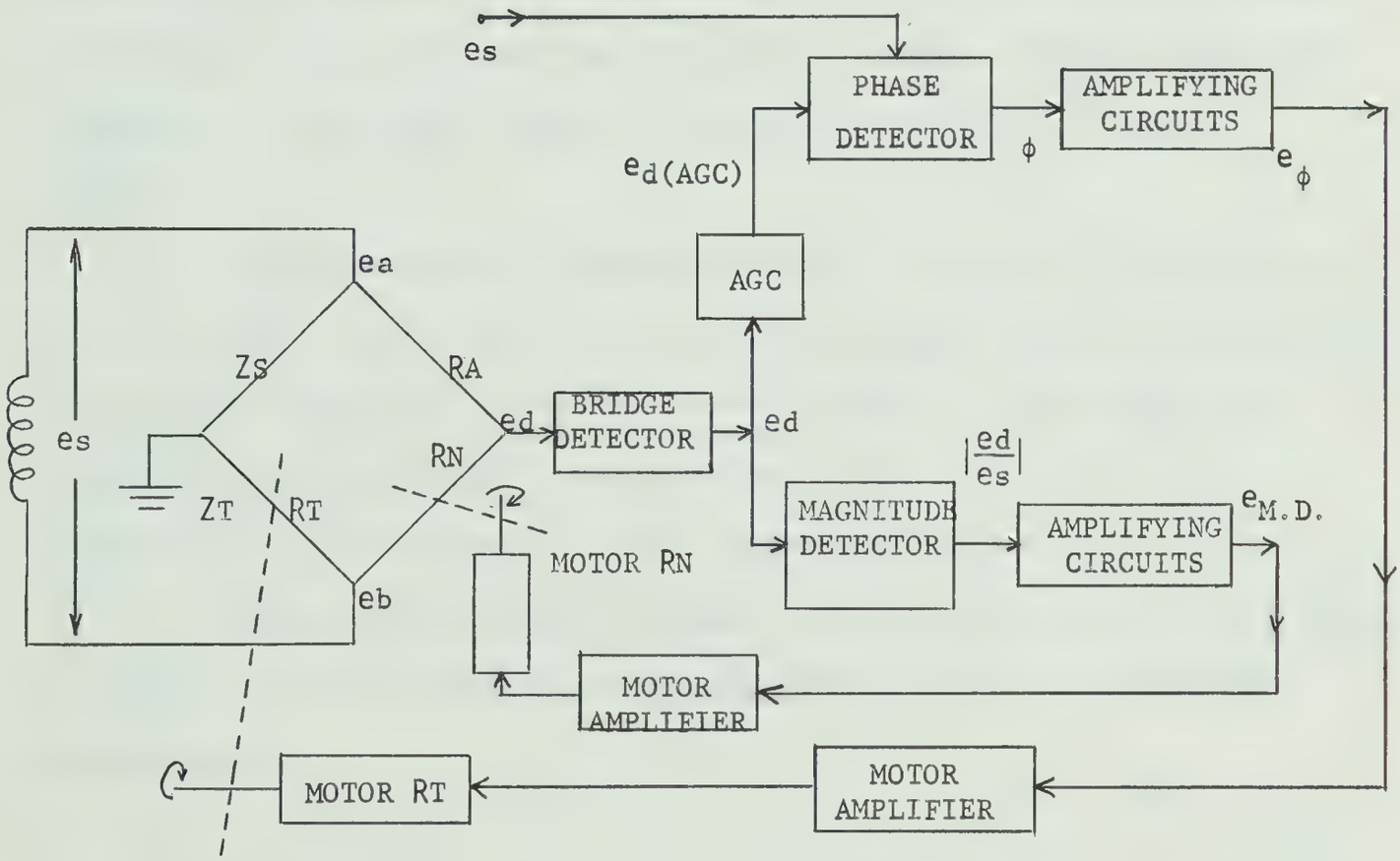


Figure 3.2 Block Diagram of the Main Circuits





A saturating characteristic yields an expanded region about the origin without overloading the subsequent circuits when e_d is large. The amplifying circuits produce an output which has a suitable magnitude for driving the power amplifier, in addition to providing a place for compensation networks to be included if necessary. The proper polarity for $e_{m.d.}$ is also derived in these and other circuits.

The power amplifier produces a 400Hz output signal whose RMS value is proportional to the D.C. input. Both power amplifiers are basically the same.

The AGC circuit is required since e_d is very small as balance is approached. It produces a 1KHz output which does not decrease appreciably until e_d is less than 1mv. The phase shift is adjustable which allows for cancellation of any phase shifts introduced in other circuits. The output impedance is low enough to drive the digital circuits in the phase detector.

The phase detector compares the zero crossings of the source (e_s) and the bridge output (e_d) and produces a pulse whose duration is equal to this time difference. Also included is a means of determining the polarity of the phase angle. The amplifying circuits have the same purposes as their counterparts in the magnitude detector.

The motors are coupled through suitable gear trains to the rheostat. A single turn 466 ohm rheostat is used for R_T; R_N is a ten turn 10,000 ohm rheostat.

CHAPTER 4

CIRCUIT DESCRIPTIONS

Other required circuits, in addition to the basic ones indicated in figure 3.2, are essential to insure the compatibility of outputs with inputs. This includes removing television, 60 Hz and 400 Hz pickup from the bridge output; converting the information from the phase and magnitude detectors into useable D.C. voltages; providing the proper polarities; and providing adequate amplification of all signals. Also necessary are 400 Hz modulators to convert the outputs of the two detectors into the proper form for the motors; and circuits forproperly sequencing the motor operations.

4.1 BRIDGE DETECTOR

The bridge detector (figure 4.1) is a very high input impedance circuit having low enough output impedance to drive the phase and magnitude detectors. Since the bridge is effectively A.C. coupled to ground, a resistor (figure 4.1) from the positive input to ground is necessary to properly bias the input transistors of the operational amplifier. To increase the effective value of this resistor, as seen at the input, feedback is applied from the output through a blocking capacitor which has negligible impedance at 1KHz. The op-amp is a Fairchild integrated circuit (μA 709). The circuit diagram and the specifications for the 709 are given in Appendix 2.

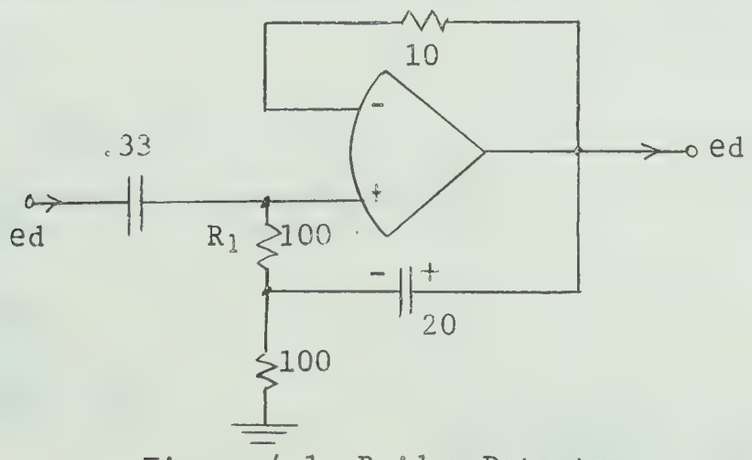


Figure 4.1 Bridge Detector

The input impedance is given approximately by:

$$ZIN \simeq R1\ (A_{O.L.}). \qquad (A_{O.L.} = \text{open loop gain of the op-amp.}) \qquad (4.1)$$

For a typical $A_{O.L.}$ of 45,000, ZIN would be 4,500 Mohms. This is in parallel with the common mode input impedance, which would be over 100 Mohms. The output impedance would be approximately equal to $(\frac{RO}{A_{O.L.}})$ where RO, typically 150 ohms, is the open loop output impedance of the op-amp.

The input capacitor protects the 709 from any voltage which may accidentally be applied to the output connector, to which the input of figure 4.1 is connected.

4.2 AUTOMATIC GAIN CONTROL (A.G.C.)

The phase detector employs two comparators to convert sine waves into square waves such that their edges coincide with the sine wave zero crossings. It is extremely difficult to adjust a comparator so it will trigger at exactly zero volts. This results in a slight time delay between the zero crossing and the edge of the square wave. The time delay is inversely proportional to the sine wave amplitude, hence large errors result when the sine wave is very small. For these reasons an A.G.C. circuit is necessary to keep the input to the phase detector reasonably constant over a wide range of ed. The scheme eventually used is shown in figure 4.2.

Amplifier A1 is a high Q active band pass filter for the purpose of removing as much noise as possible from the bridge output. The transfer function[2] is:

$$G_1 = -\frac{(\frac{1}{R_1C_4})\ S}{S_2 + S\frac{1}{R_5}(\frac{1}{C_4} + \frac{1}{C_3}) + \frac{1}{C_3C_4R_5}(\frac{1}{R_1} + \frac{1}{R_2})} \qquad (4.2a)$$

$$= -\frac{A_o\ (\frac{\omega_o}{Q})S}{S^2 + (\frac{\omega_o}{Q})S + \omega_o^2} \qquad (4.2b)$$

ω_o = resonant freezing
A_o = resonant gain
Q = quality factor.

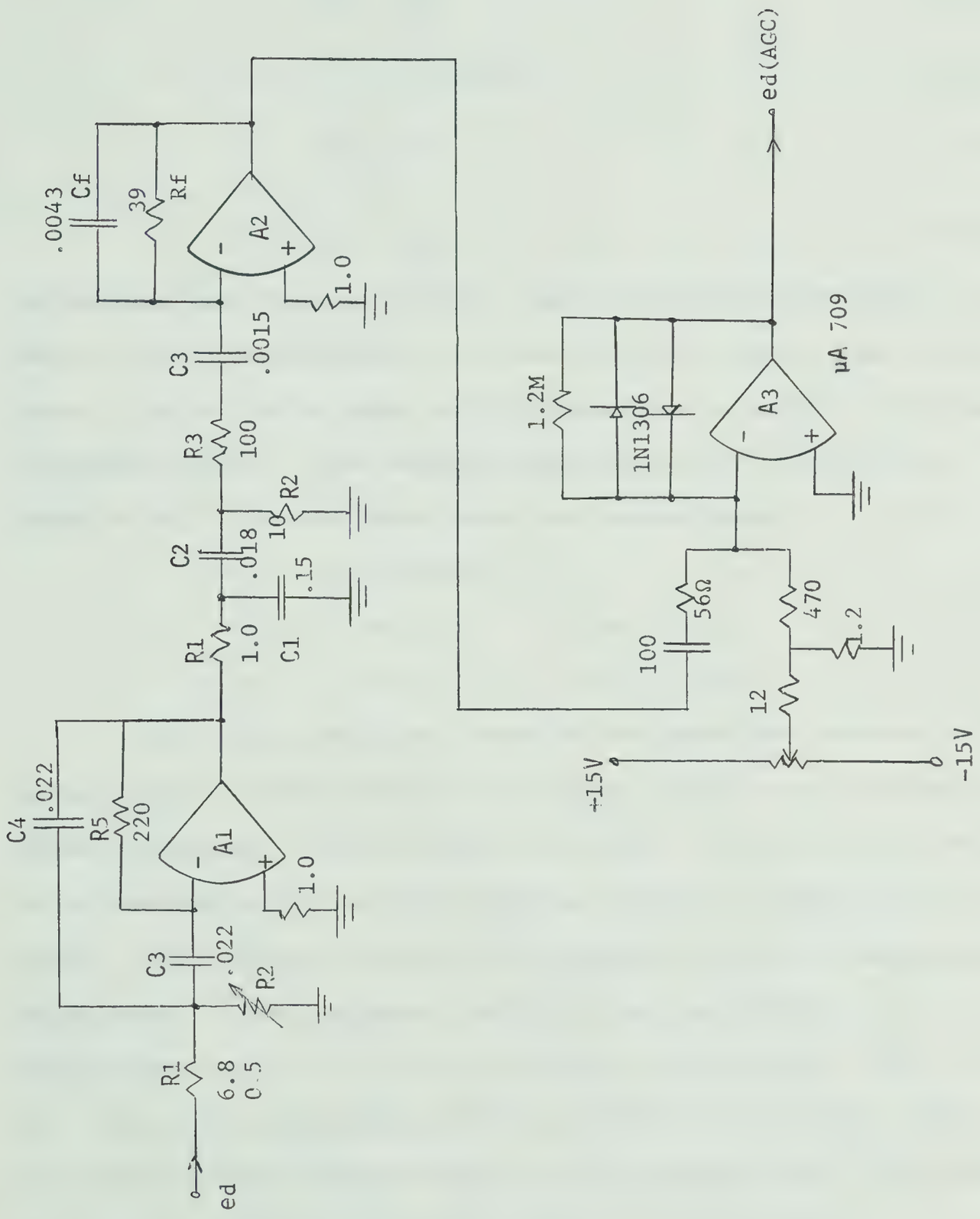


Figure 4.2 A. G. C. Circuit

The design equations for this filter are obtained by equating the coefficients in equations 4.2a and 4.2b. For ease of calculations, C_3 and C_4 are made equal.

$$R_1 = \frac{Q}{A_o \kappa} \tag{4.3}$$

$$R_2 = \frac{Q}{\kappa} \cdot \frac{1}{2Q^2 - A} \tag{4.4}$$

$$R_5 = \frac{2Q}{\kappa} \tag{4.5}$$

$$C = \frac{\kappa}{\omega_o} \tag{4.6}$$

The constant κ is chosen arbitrarily, and establishes the impedance levels. Resistor R_2 is made variable so that the filter is tunable over a small range. This allows the phase shift between input and output to be adjusted accurately to 180.0°. The measured characteristics of the filter are listed below. (The calculated values are in parentheses.)

ω_o = 1010 Hz

A_o = 12.2 (A_o = 16.1)

$Q \simeq 11.2$ (Q = 13.9)

When this circuit was tested, it was noted that there was an output signal of random amplitude (<1 mV peak to peak) at approximately the resonant frequency, when the input was grounded. This was attributed to noise generated in the amplifier which was filtered to produce the observed output. The amplitude appeared to be independent of Ao, but was nevertheless large enough to cause erroneous results in the phase detector. By introducing a gain of 12.2 in the filter and an attenuation of 12.2 in the next stage, the noise signal would be reduced by the same ratio, whilst the original signal would be restored to its original level. This method effectively eliminated the harmful effects of the noise signal.

Amplifier A_2 is a broad band pass active filter (i.e. no resonant peak) whose reponse falls off at 40 db per decade on each side of

the center frequency. The transfer function is given approximately by:

$$G_2 \simeq \frac{S^2T_2C_3R_f}{(1 + ST_1)(1 + ST_2)(1 + ST_3)(1 + ST_4)} \qquad (T = RC) \qquad (4.7)$$

$$(R_1 << R_2 << R_3)$$
$$(C_1 >> C_2 >> C_3)$$

The gain at the center frequency is .082 ($\simeq \frac{1}{12.2}$). The time constants are all equal and are such that the center frequency is close to 1KHz when standard components are used.

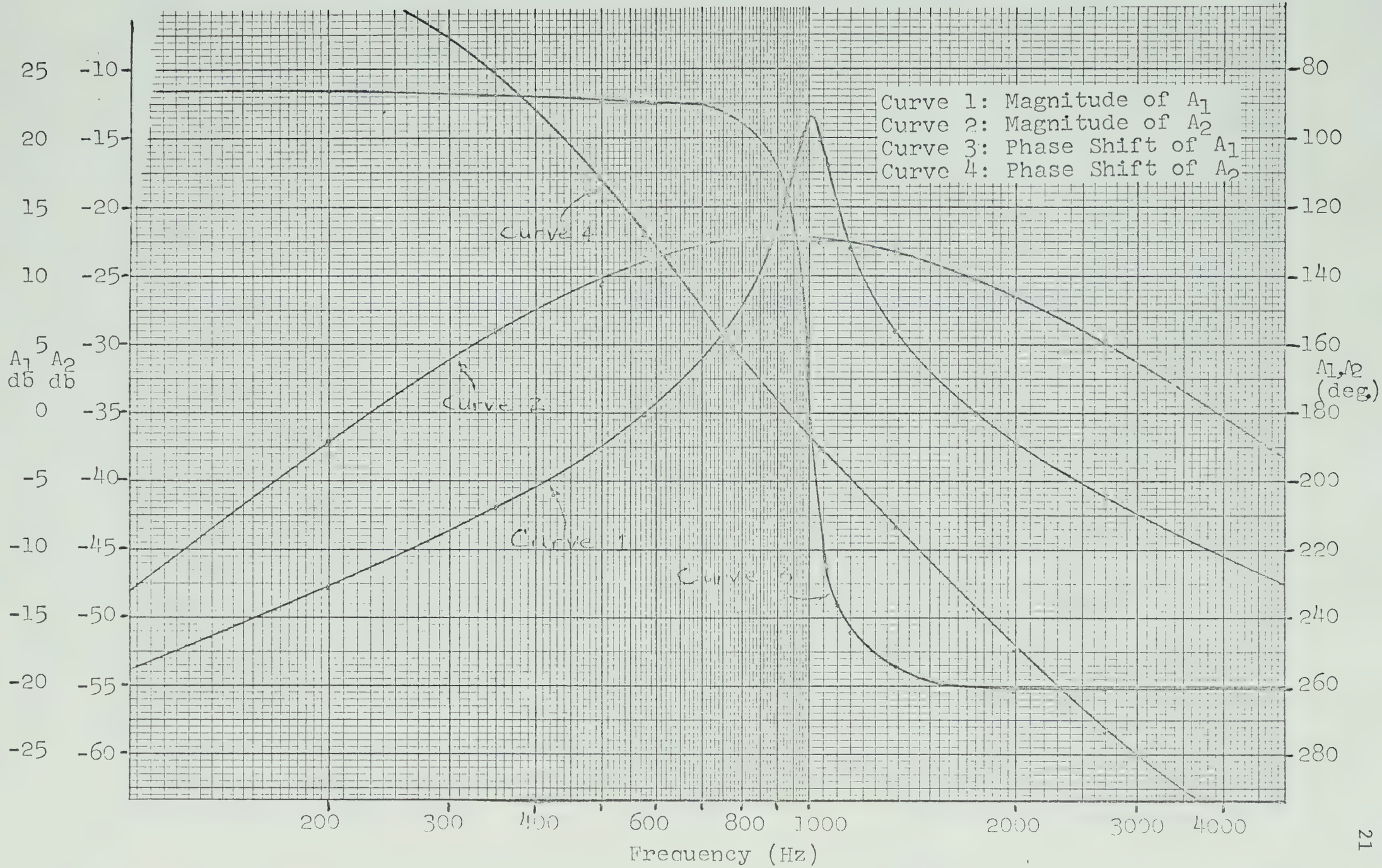
The experimental magnitude and phase angle characteristics of A_1 and A_2 are illustrated in Graph 1. Graph 2 is the magnitude characteristic with the filters cascaded.

Amplifier A_1 has a saturating characteristic having a very high gain when the output is less than the diode voltages. The output is limited to about $\pm$ 0.6 volts by the diodes. Capacitor C_1 blocks any D.C. offset from A_2, and resistor R_f provides D.C. feedback to reduce the D.C. drift of the output voltage. The resistive network on the input allows removal of any offsets in the amplifier. A high performance integrated circuit (709) was used to provide the high gain and stable temperature characteristics required.

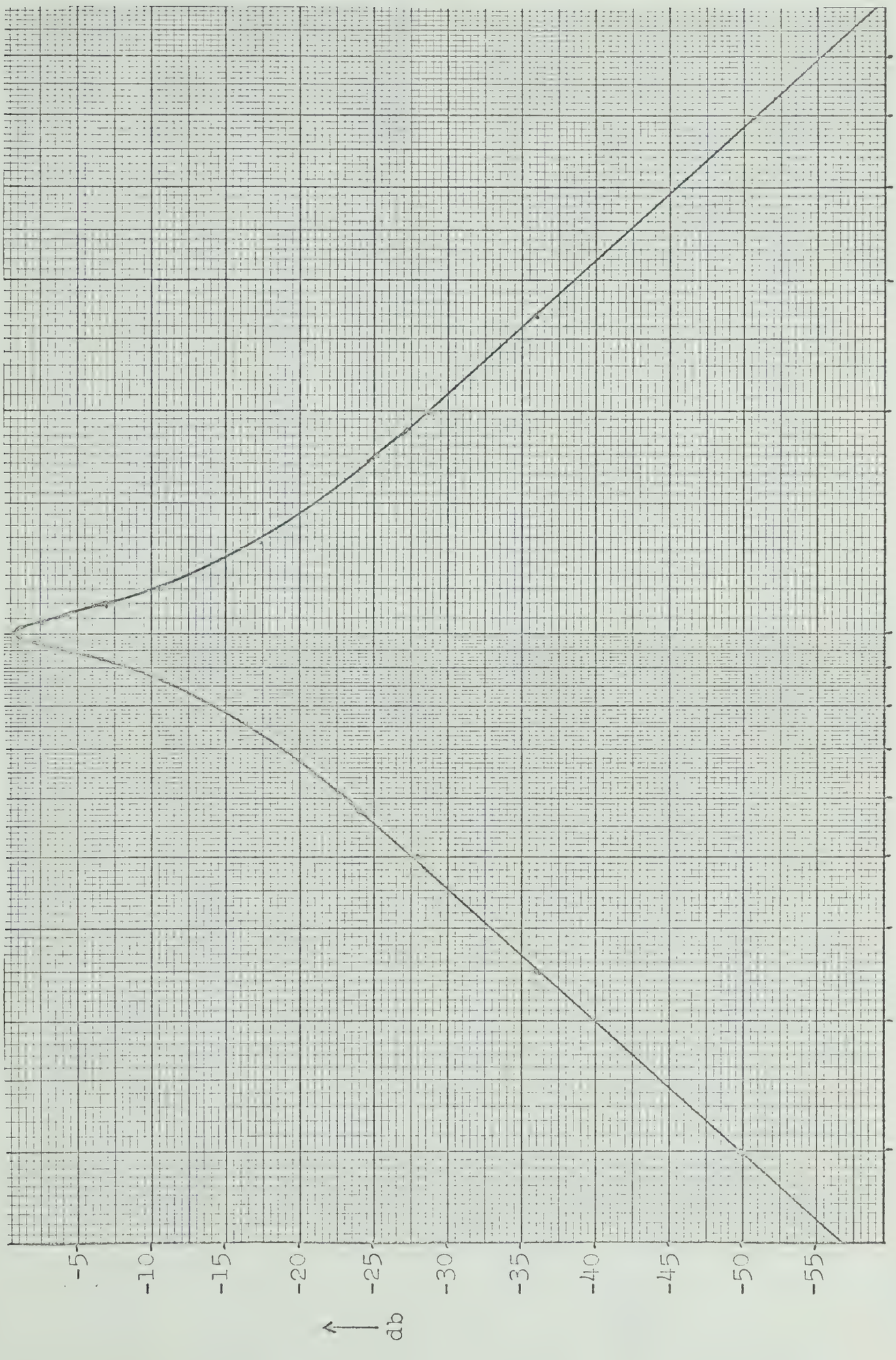
4.3 PHASE DETECTOR

The main portion of the phase detector is shown in figure 4.3. The comparators, which are Fairchild integrated circuits μA710 (Appendix 3) connected as Schmitt triggers, convert the sine wave inputs to square waves, whose edges coincide with the zero crossings of the input.

The threshold voltages are made adjustable by the potentiometers, and the amount of hysteresis is controlled by the ratio of R_f and R_i. The two resistors, R_1, are made equal to minimize the temperature drift of the threshold voltages due to changing bias currents. Hysteresis in the



Graph 1 Experimental Magnitude and Phase Angle Curves of A_1 and A_2 (Figure 4.2)



Graph 2 Magnitude Curve of Cascaded Filters (Figure 4.2)

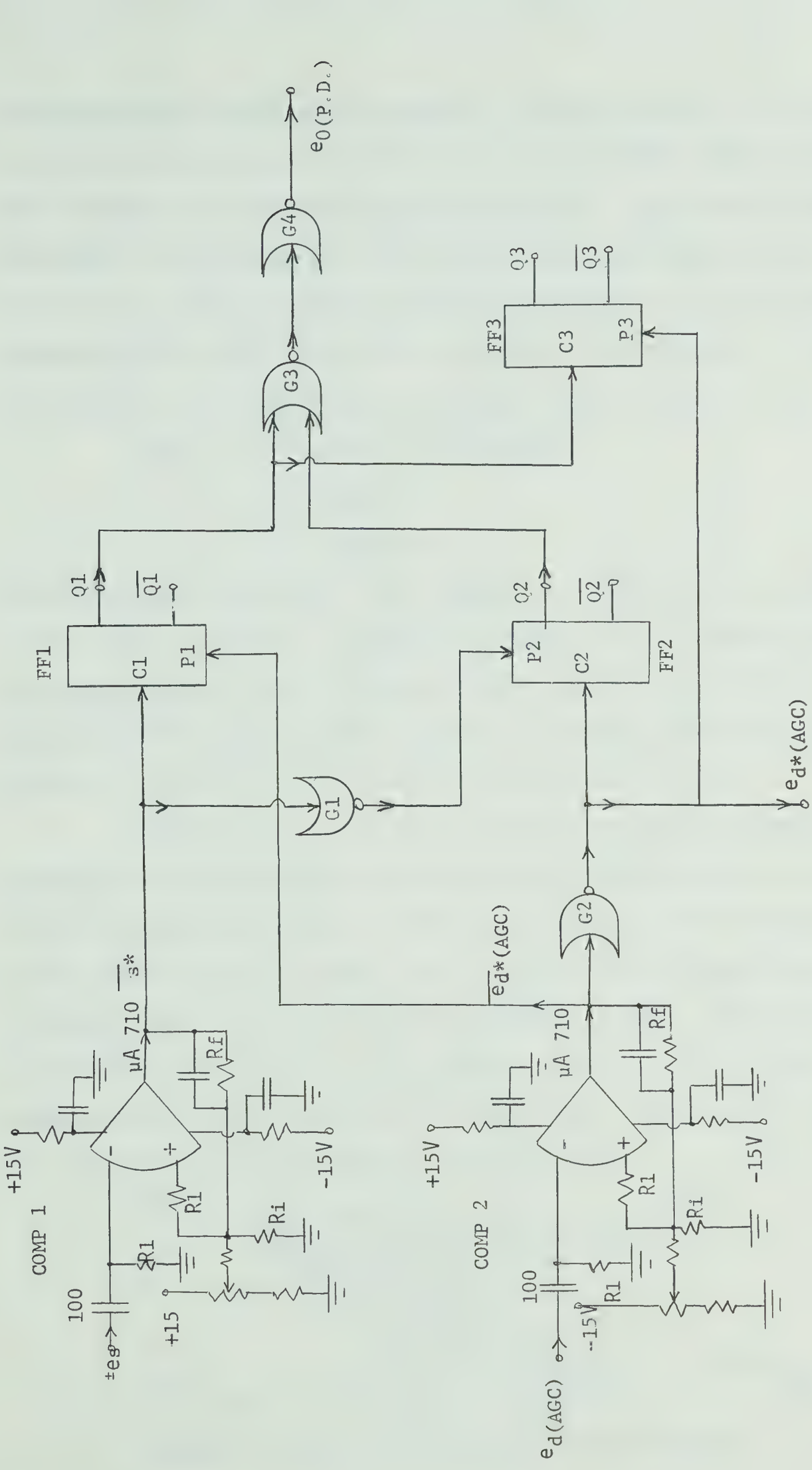


Figure 4.3 Phase Detector

switching points requires that comparator 1 (COMP 1) switch at the zero crossing on the rising part of the input; and that COMP 2 switch at the zero crossing on the falling part of the waveform. The comparator outputs are applied to flip-flop 1(FF1) such that one reference edge turns the flip-flop on, while the other reference edge turns it off. When the two signals are 180° out of phase, the two reference edges coincide. Hence the flip-flop is not turned on and the output stays at zero.

Figure 4.5 illustrates two conditions:

(1) - ed lagging es

(2) - ed leading es

FF1 has an output only when - ed is lagging es (condition #1). For this reason, FF2 is required. The signals are applied to it, such that it has an output only when - ed is leading es (condition #2). Gating the output signals of these two flip-flops result in a rectangular wave whose time duration is proportional to the phase angle between - ed and es.

Since the output of G4 is positive for positive and negative values of ϕ, additional logic is required to provide polarity information. This is accomplished, in part, by FF3. For condition 1, the falling edge of Q1 puts Q3 to the "1" state, and the rising edge of G2 (the falling edge of COMP 2) sets it to the "0" state one half cycle later. This results in a square wave output for FF3. For condition 2, Q1 is zero so that Q3 remains at zero due to pulses on the preset input. The circuit in figure 4.4 converts the output of FF3 into a useable form.

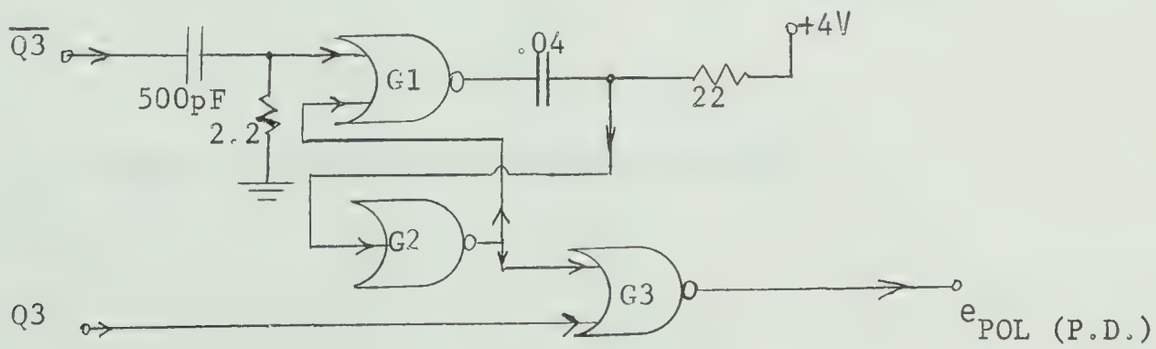


Figure 4.4 Polarity Conversion for Phase Detector

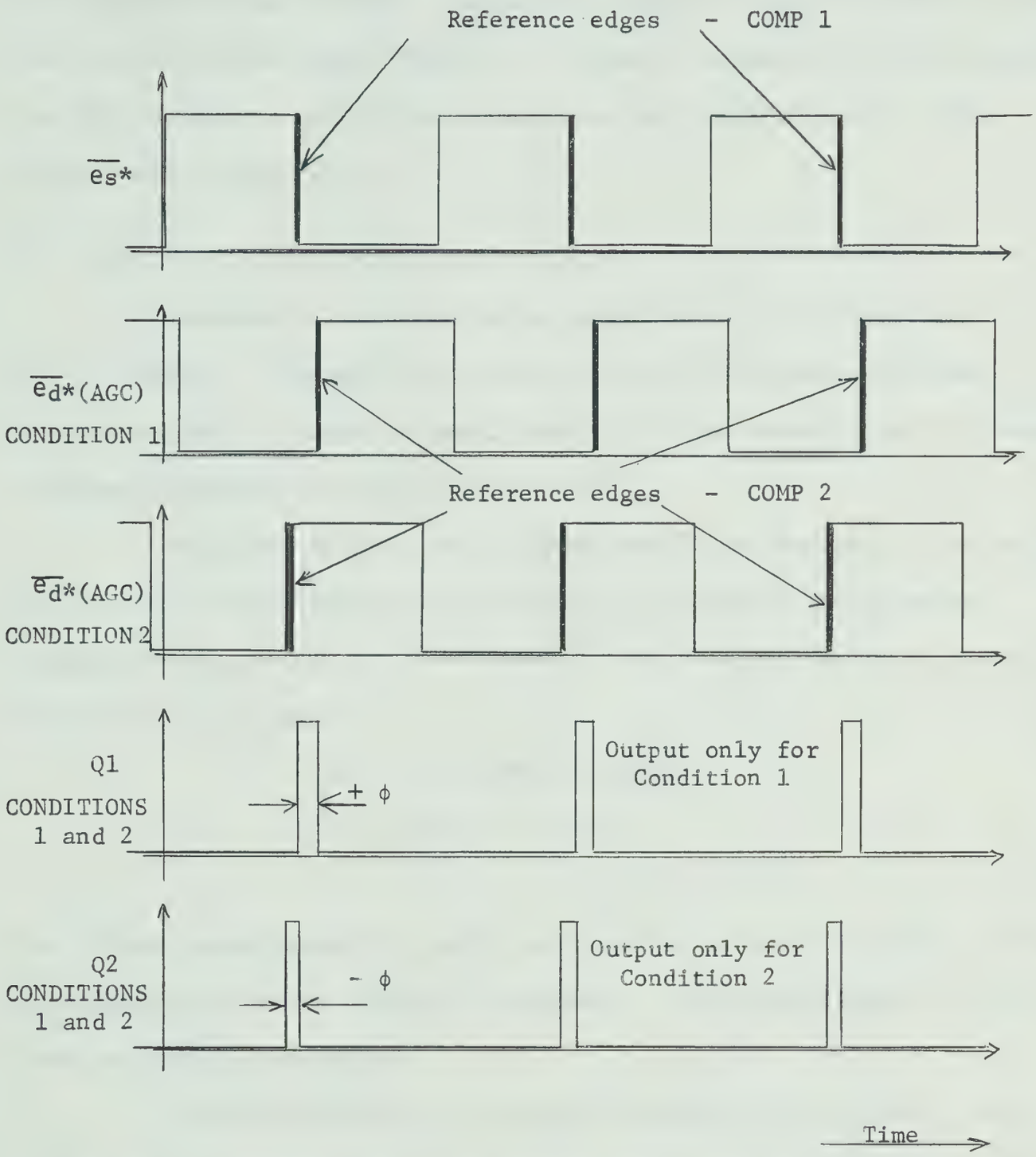
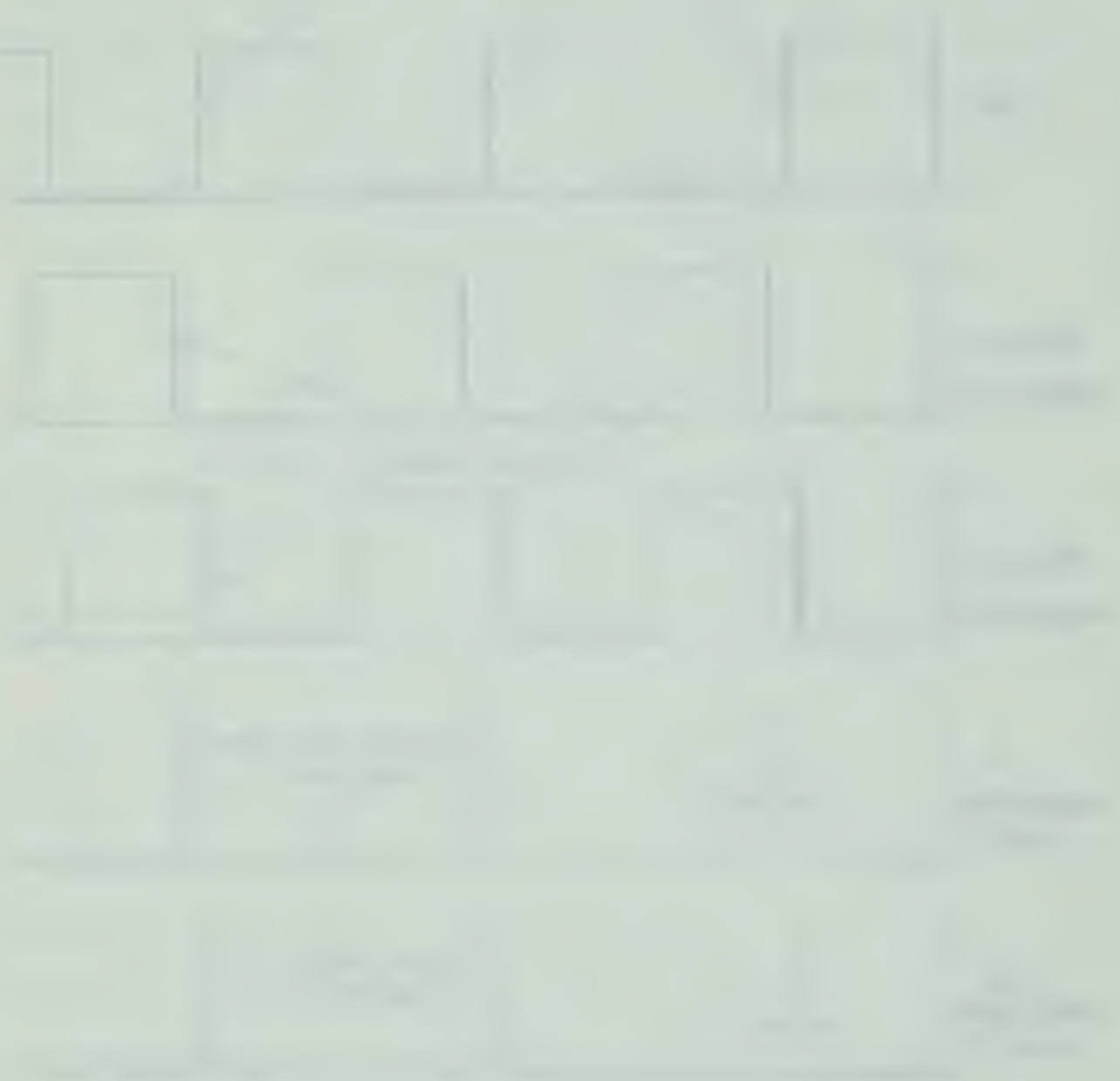


Figure 4.5 Waveforms in Phase Detector



G1 and G2 are connected to form a monostable multivibrator. It is triggered by positive pulses generated from the leading edges of $\overline{Q3}$ by the differentiating network. The output pulse is slightly longer than half the period of $\overline{Q3}$ so that $e_{POL(P.D.)} = 0$ when G2 is gated with Q3 (condition 1). For $\overline{Q3}$ a constant, both G2 and G3 are zero and $e_{POL(P.D.)} = 1$. This corresponds to condition 2.

4.4 AMPLIFYING CIRCUITS FOR PHASE DETECTOR

The gain of the phase detector in figure 4.3 is very low ($A \simeq 8$ mV/deg). To amplify this output without introducing problems related to the D.C. drift of amplifiers, it is converted to an A.C. signal, then amplified and rectified (figure 4.6).

Amplifier A_1 is an active band pass filter similar to the one used in the AGC circuit (figure 4.3). Graph 3 is a plot of the phase and magnitude characteristics of A_1. From it are obtained the experimental values of ωo, Ao, and Q.

$$\omega o = 0.95 \text{ KHz } (.915 \text{ KHz})$$

$$Q \simeq 8.3 \qquad (9.4)$$

$$A = 6.2 \qquad (7.7)$$

The 5 Kohm potentiometer is used to adjust the resonant frequency, and also to adjust the gain (at 1 KHz) if necessary. The output signal is a sine wave with little distortion.

The signal from A_1 is full wave rectified by A_2 and A_3. The diodes in the feedback loop of A_2 provide half wave rectification, with the hysteresis of the diodes reduced by a factor equal to the open loop gain of A_2. By summing the input and output of A_2, with proper weighting factors, in A_3, a fully rectified wave results. The filter at the input of A_2 provides additional filtering; while the resistive network at the positive input is a zero adjustment to permit rectification of signals as small as 2 mV (P/P).

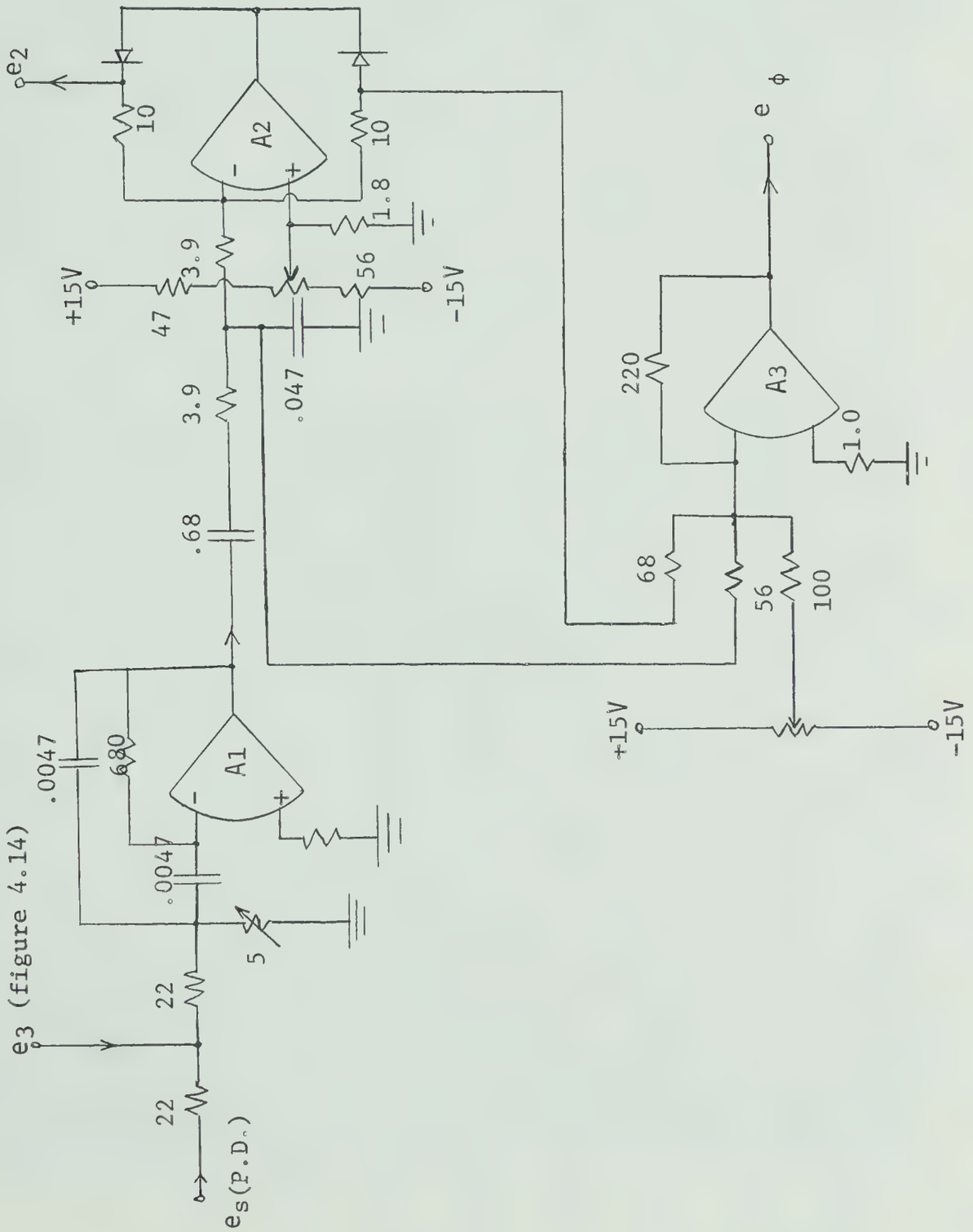
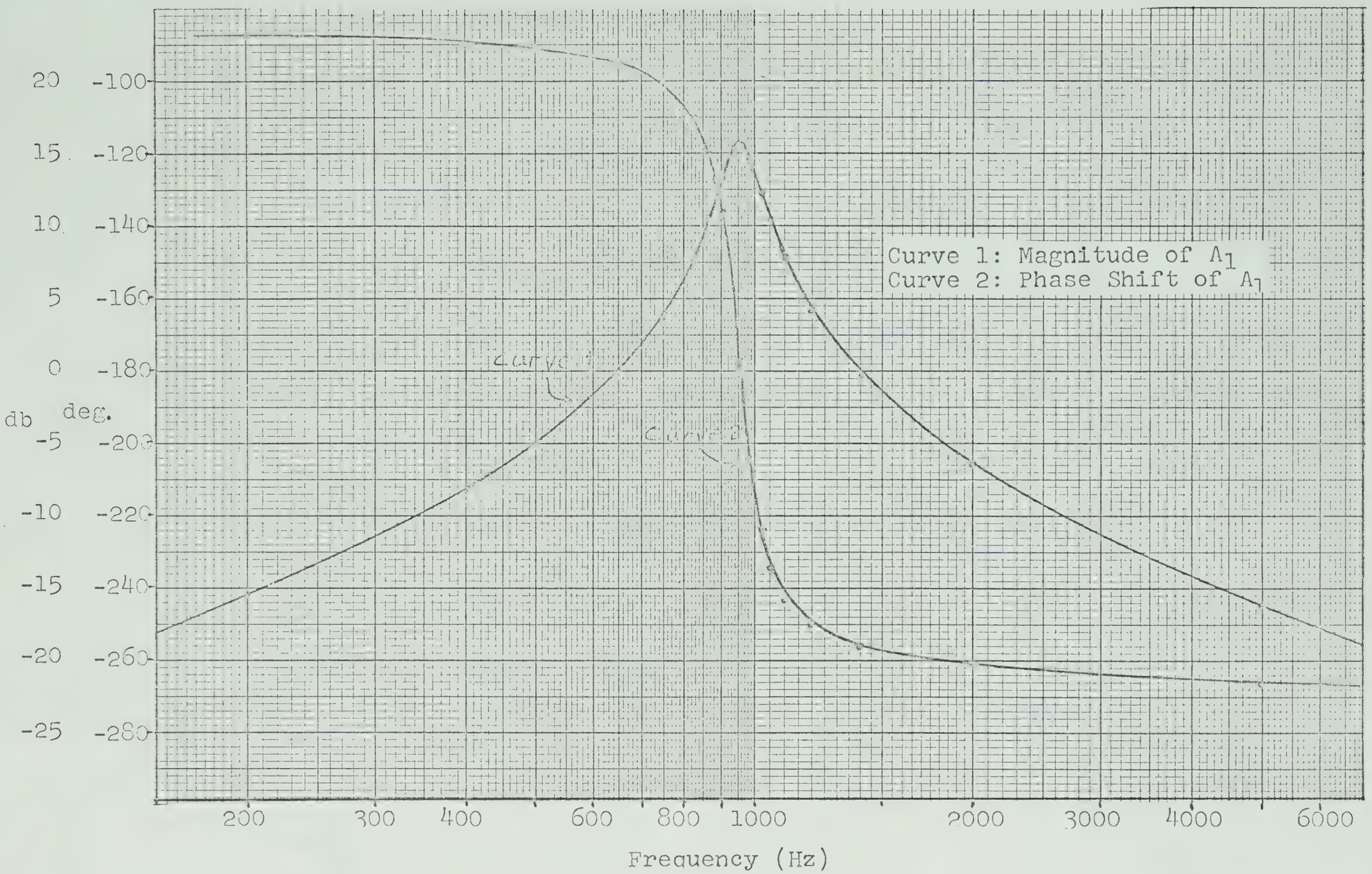


Figure 4.6 Amplifiers for Phase Detector





Graph 3 Experimental Magnitude and Phase Angle Curves of A_1 (Figure 4.6)

The biasing network at the input of A_3 permits a D.C. voltage to be added to the output which reduces the effective deadzone in the servomotor. The signal e_3 is actually a transistor switch. Under certain conditions (explained later in the chapter) the input to motor RT is removed. Since the phase angle information is no longer required, the amplifiers in figure 4.6 are made inactive by shorting the input of A_1 to ground. This reduces the transient signals which are picked up by other circuits through supply lines and ground wires.

4.5 ADDITIONAL CIRCUITS FOR PHASE DETECTOR

The transfer characteristic of the phase detector $(\frac{e\phi}{\phi})$ should be similar to that shown in figure 4.7, particularly with respect to the continuity of $e\phi$ at $\phi = 0°$ and $\phi = 360°$. The present circuit does not accomplish this (figure 4.8).

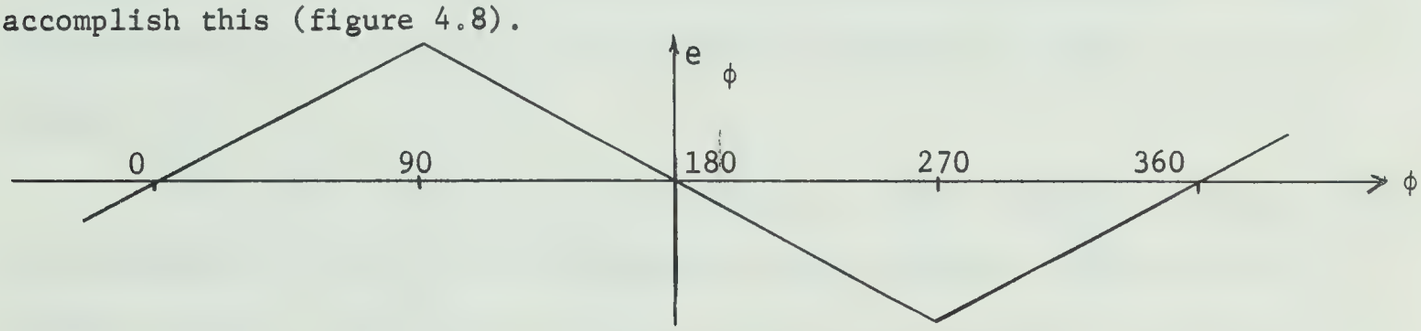


Figure 4.7 Required Transfer Characteristic

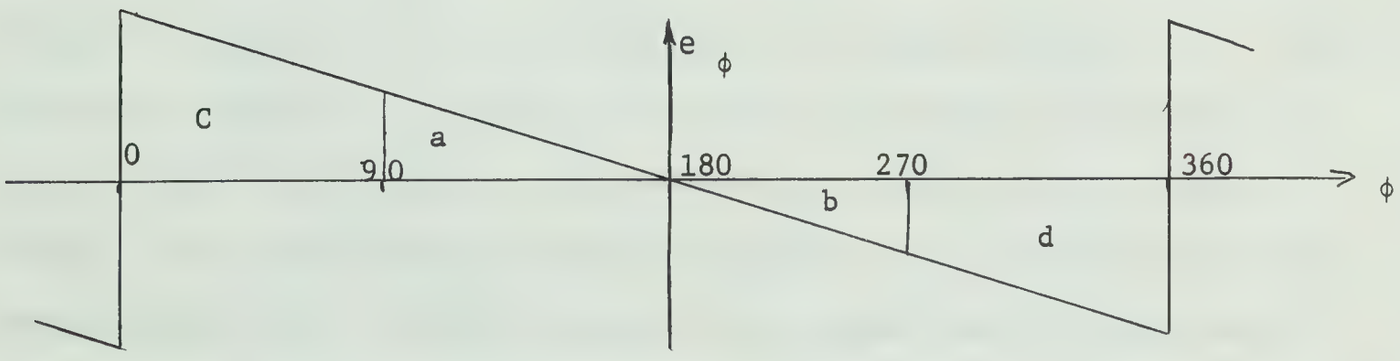


Figure 4.8 Transfer Characteristic of Figure 4.3

The proper operating region of the circuitry should occur in regions 'a' and 'b'. By inverting one of the phase detector inputs (es) when regions 'c' and 'd' are reached, the effective angle changes by 180°, and these regions are transformed into 'b' and 'a' respectively. For example $\phi = 80°$ changes to $\phi = 80 + 180 = 260°$; and $\phi = 300°$ changes to $\phi = 300 - 180 = 120°$. This yields the curve illustrated in figure 4.9.

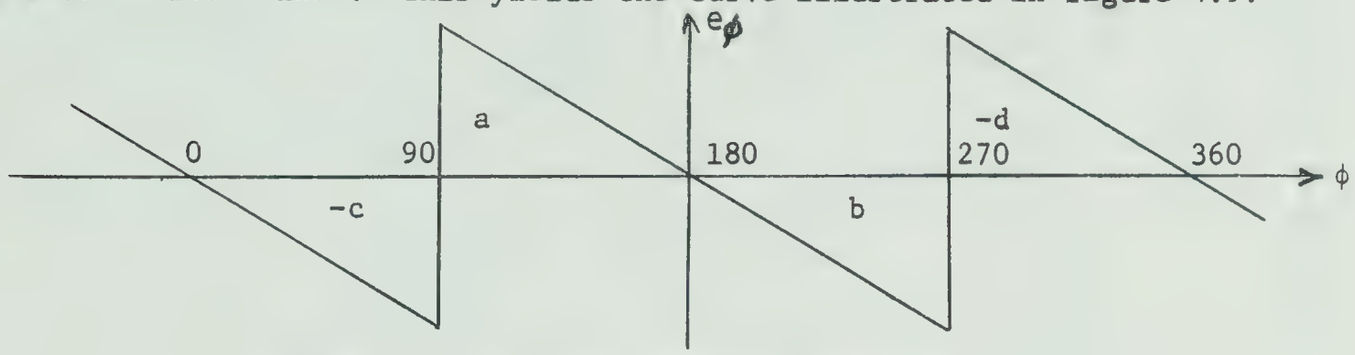


Figure 4.9 Modified Transfer Characteristic

The proper continuity has been obtained, but it results in the wrong polarity in regions -c and -d. This is corrected by reversing the polarity of $e\phi$ at the same time es is inverted. The circuitry required for this is shown in Figure 4.10.

The input (e_2) is a half wave which is taken from A_2 in figure 4.6. It is buffered by a high input impedance emitter follower with a gain of slightly over 1. The low pass filter produces a D.C. output proportional to e_2, which is suitable for triggering the Schmitt trigger. The Schmitt trigger is adjusted so it will switch when ϕ is between 100° and 120°. This causes the flip-flop to change states which, at the same time, inverts the output of the source detector, and reverses the polarity for the polarity switch. The summing amplifier adds the signals +es and -es from the source detector (only one of which is present at any given time) to yield +es or -es. The output of the amplifier is then applied to one of the inputs of the phase detector (figure 4.3).

The source detector subtracts eb from ea (figure 1.1) to obtain es.

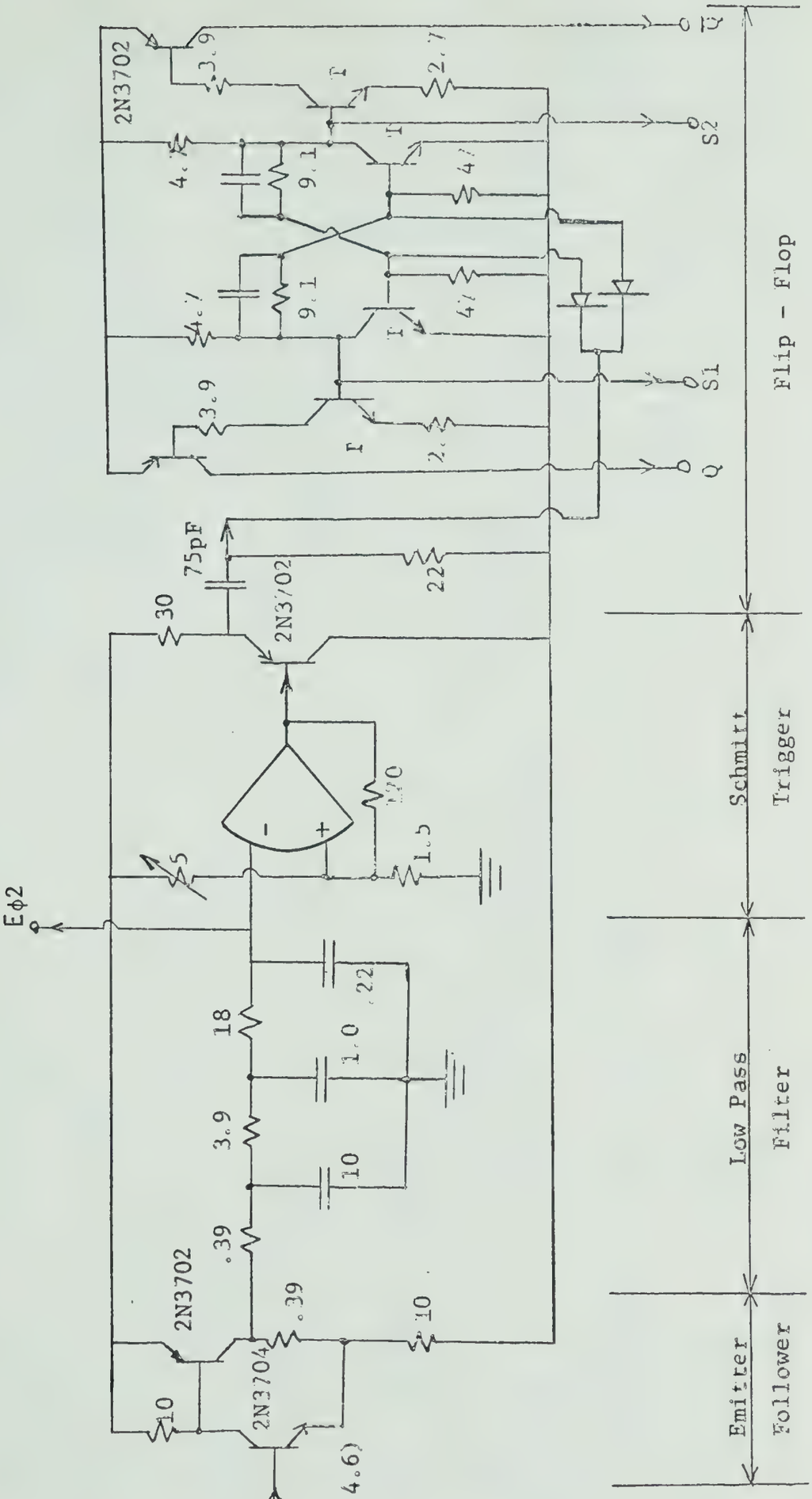
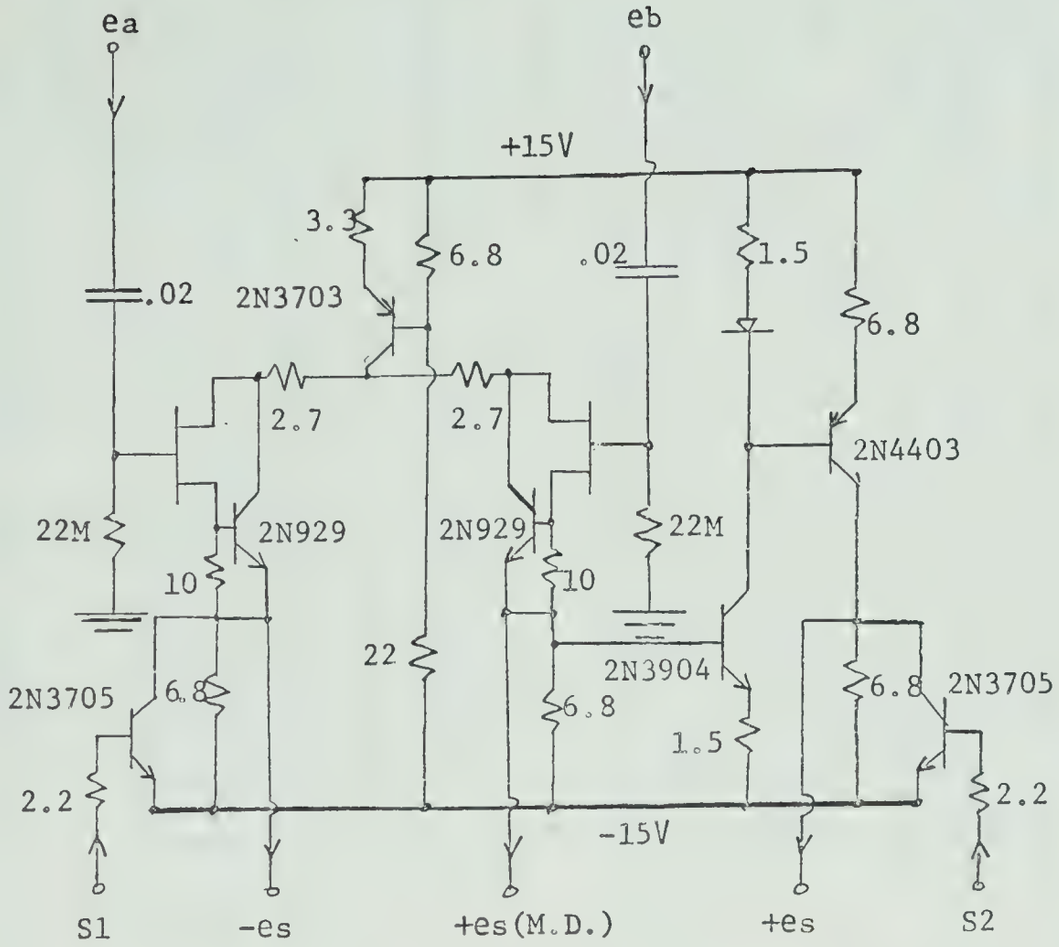
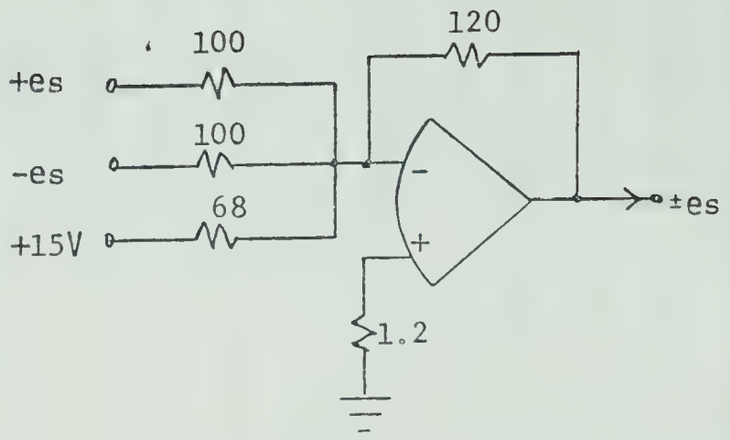


Figure 4.10(a) Additional Circuitry for Proper Transfer Characteristic

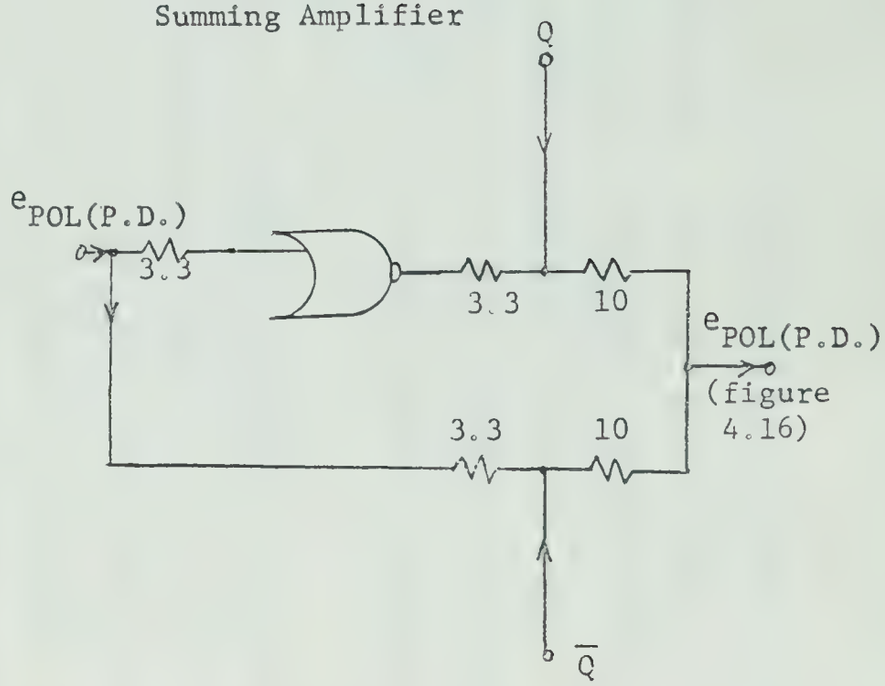


(figure 4.12)

Source Detector



Summing Amplifier



Polarity Switches

Figure 4.10(b) Additional Circuitry for Proper Transfer Characteristic

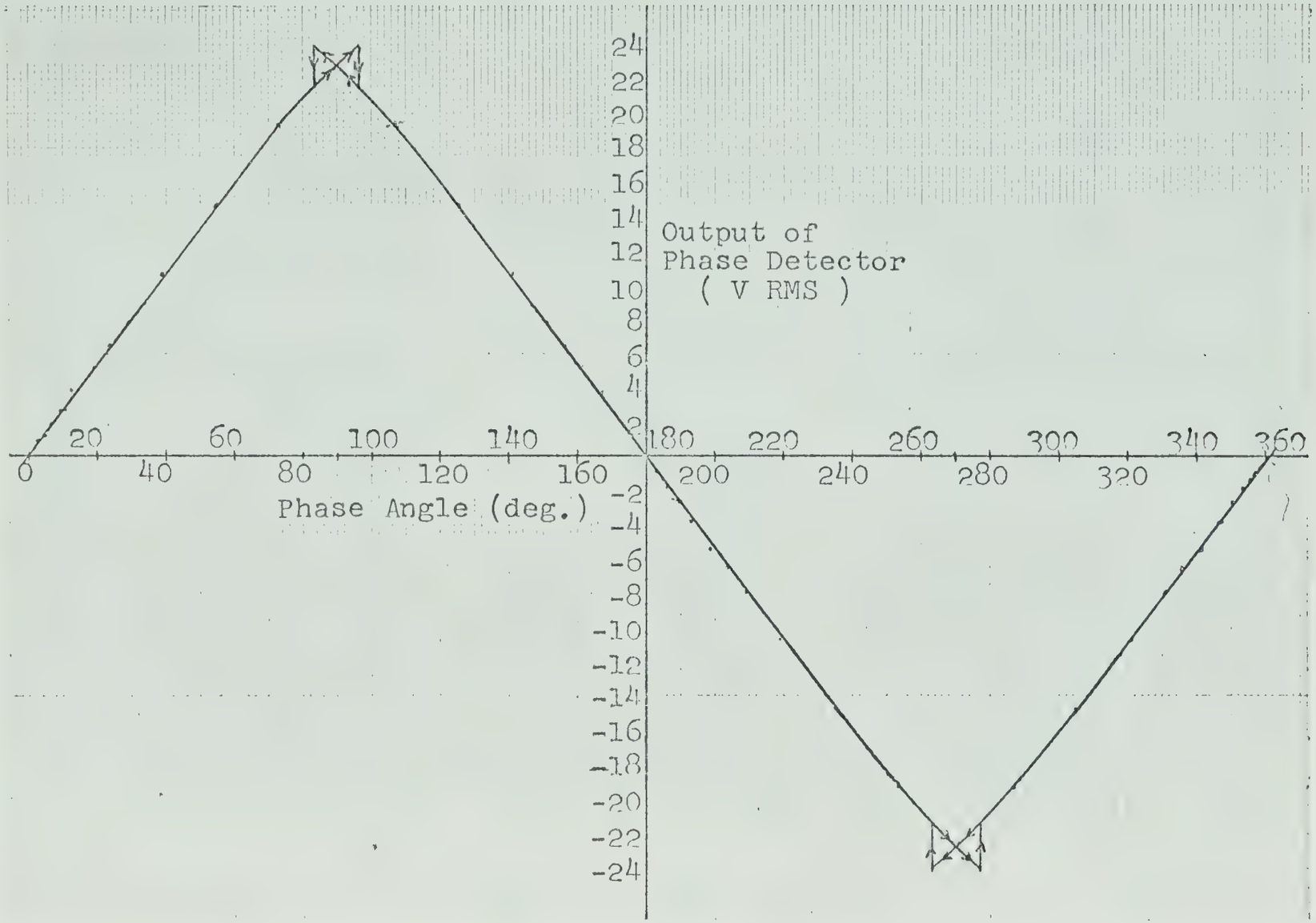
This is made necessary because of phase shift between the primary and the secondary of the coupling transformers. This phase shift depends upon the components in the bridge and hence makes the primary voltage unsuitable for the phase detector. To minimize the loading on the bridge, the differential amplifier is composed of high input impedance field effect transistors. The output, +es(M.D.), is used as an input to the magnitude detector polarity circuit (figure 4.12).

Graphs 4 and 5 indicate the important characteristics of the phase detector. The transfer characteristic (Graph 4) of the detector exhibits a gain of approximately 0.275 volts/degree in the linear region. The dotted portions of the curve indicate the projected performance under the condition that the supply voltages to A_3 are large enough to keep the amplifier from saturating. With the ± 15V power supplies, saturation occurs approximately at ± 14.5V. Graph 5 indicates how the indicated phase angle varies as the input to the detector, ed, is changed from 1.0 mV (p/p) to 1.8 (p/p) with the phase angle between the two inputs (s and d) kept at 0.0°. The maximum error is + 2.16° which occurs at e_d = 7.1 m (p/p). This is very small and under the worst conditions, assuming this were the only source of error in the bridge, would result in a maximum null voltage of ed = 0.26 mV (p/p).

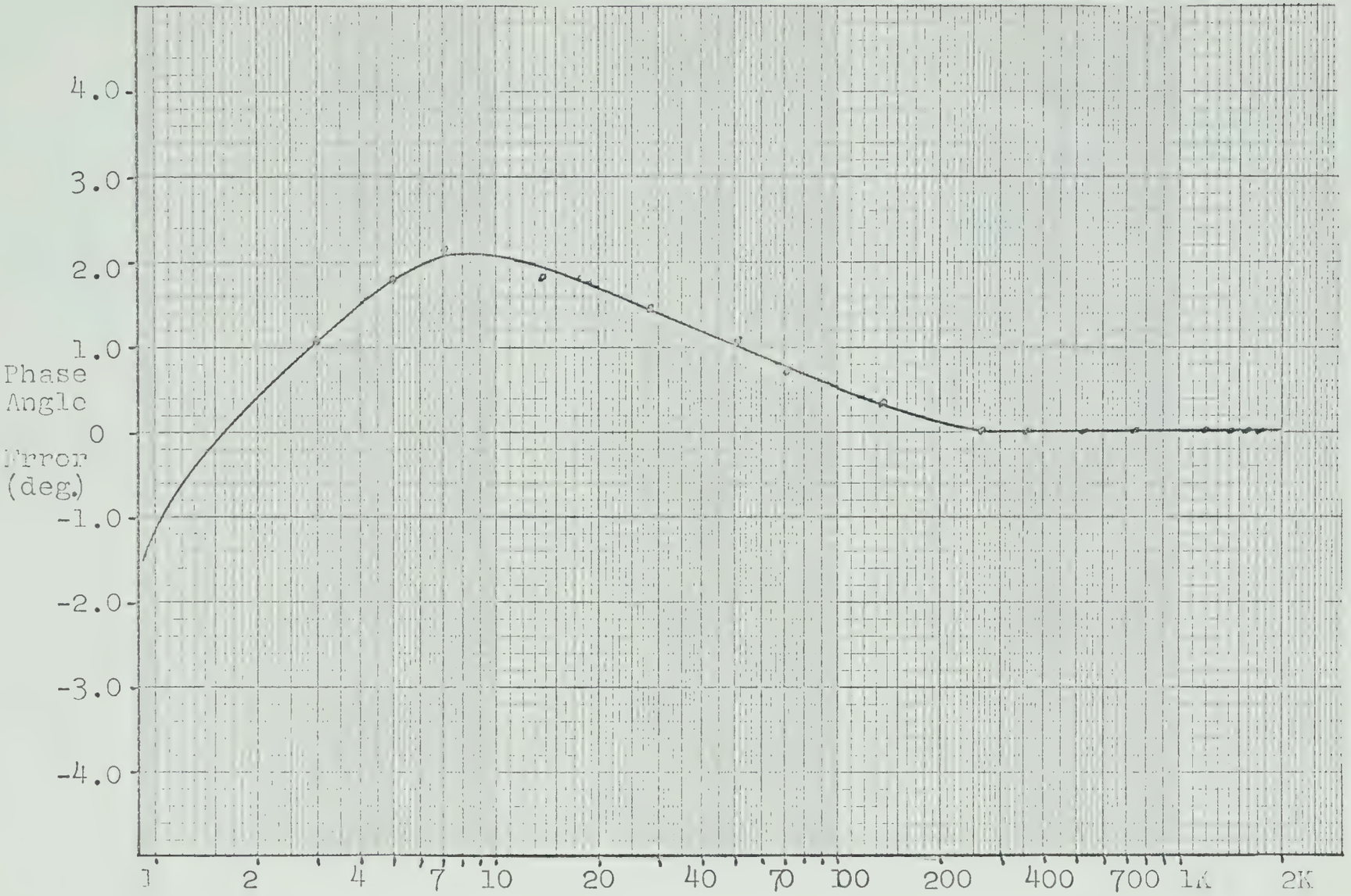
4.6 MAGNITUDE DETECTOR AND AMPLIFYING CIRCUITS

The magnitude detector is shown in Figure 4.11. Amplifier A_1 provides high amplification of ed at 1KHz and filters objectionable noise (e.g. television, 60Hz, and 400Hz). A_2 and A_3 rectify and filter the output from A_1. They also shape the transfer characteristic and provide further amplification.

The calculated transfer characteristic of A_1 (for eo < .3V p/p) is:



Graph 4 Transfer Characteristics for Phase Detector



Graph 5 Error in Phase Angle as One Input Changes Amplitude

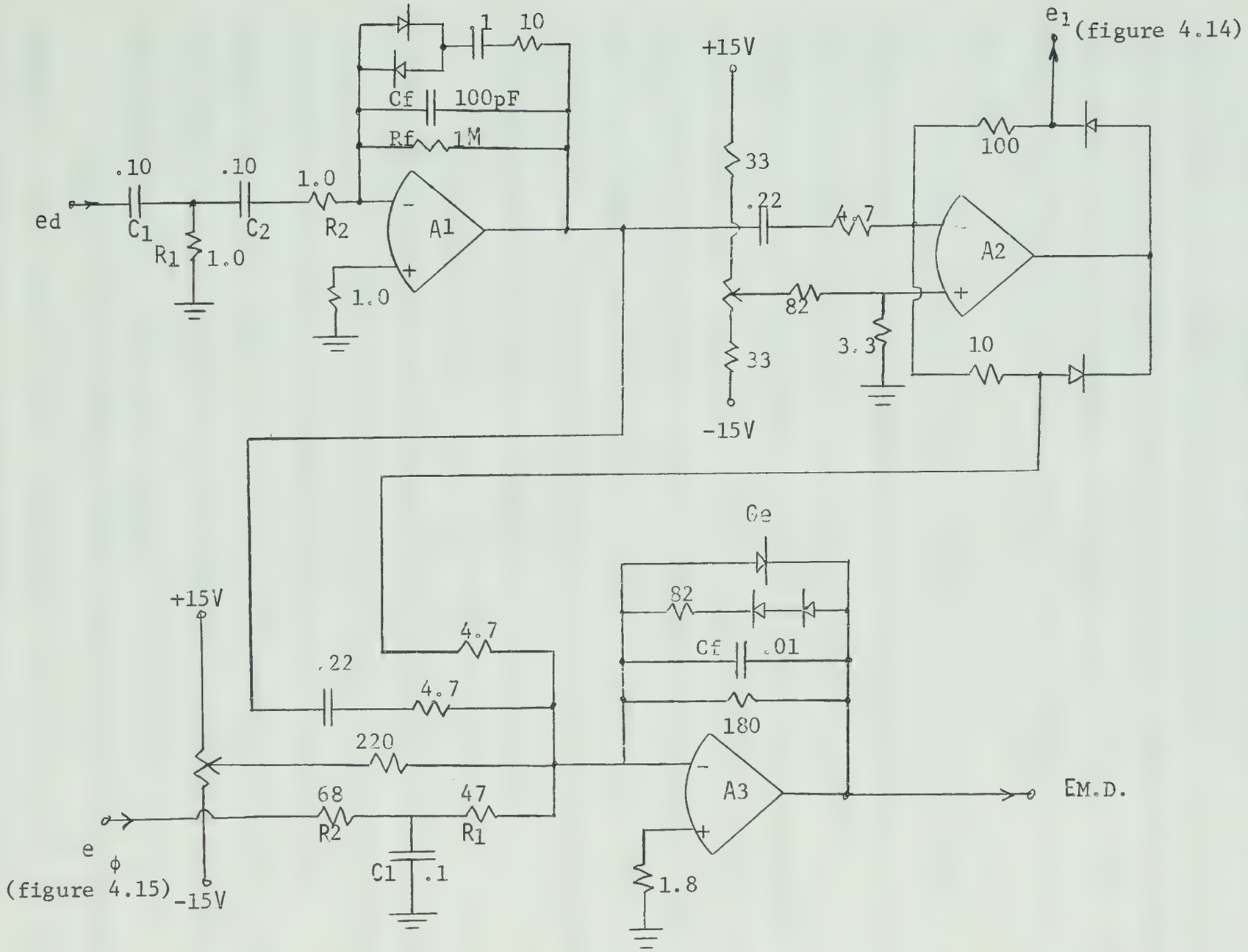


Figure 4.11 Magnitude Detector and Amplifying Circuits

$$\frac{e_o}{e_i} = \left(\frac{R_f}{1+ST_f}\right) \frac{(R_1C_1C_2)S^2}{[S^2R_1R_2C_1C_2 + SR_1(C_1 + C_2) + 1]} \qquad (4.8a)$$

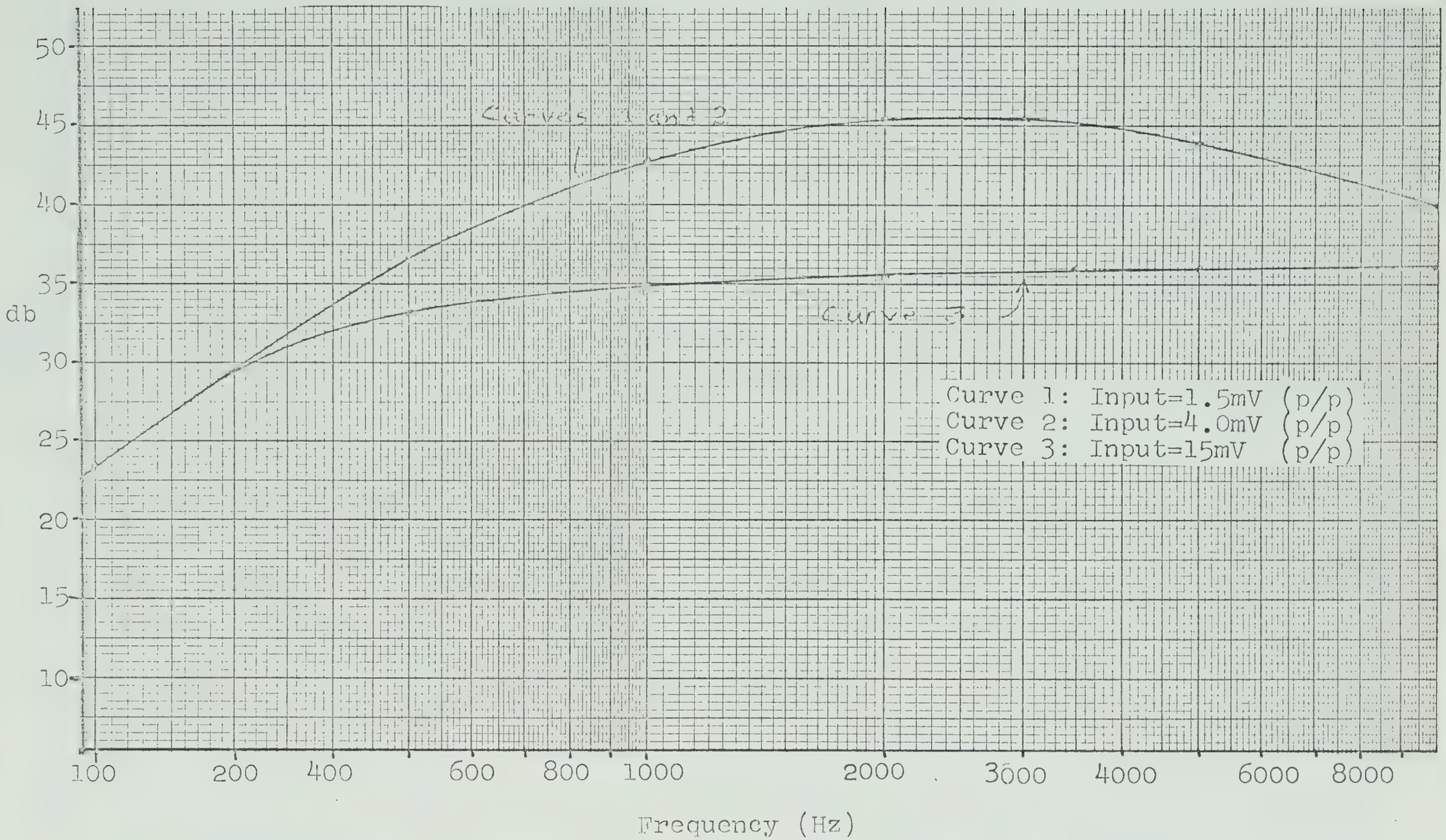
$$= \frac{10^{-5}\,S^2}{(10^{-4}S + 1)^3} \qquad (4.8b)$$

Graph 6 is the measured magnitude characteristics of A_1 for three values of input. The center frequency has deliberately been selected as 1.6 KHz so that the relative attenuation of the 50 Hz and 400 Hz signals, with respect to 1 KHz, is greater. The gain of A_1 at 1 KHz is 138 (= 42.8db). The output waveform is sufficiently free of noise to require no further filtering.

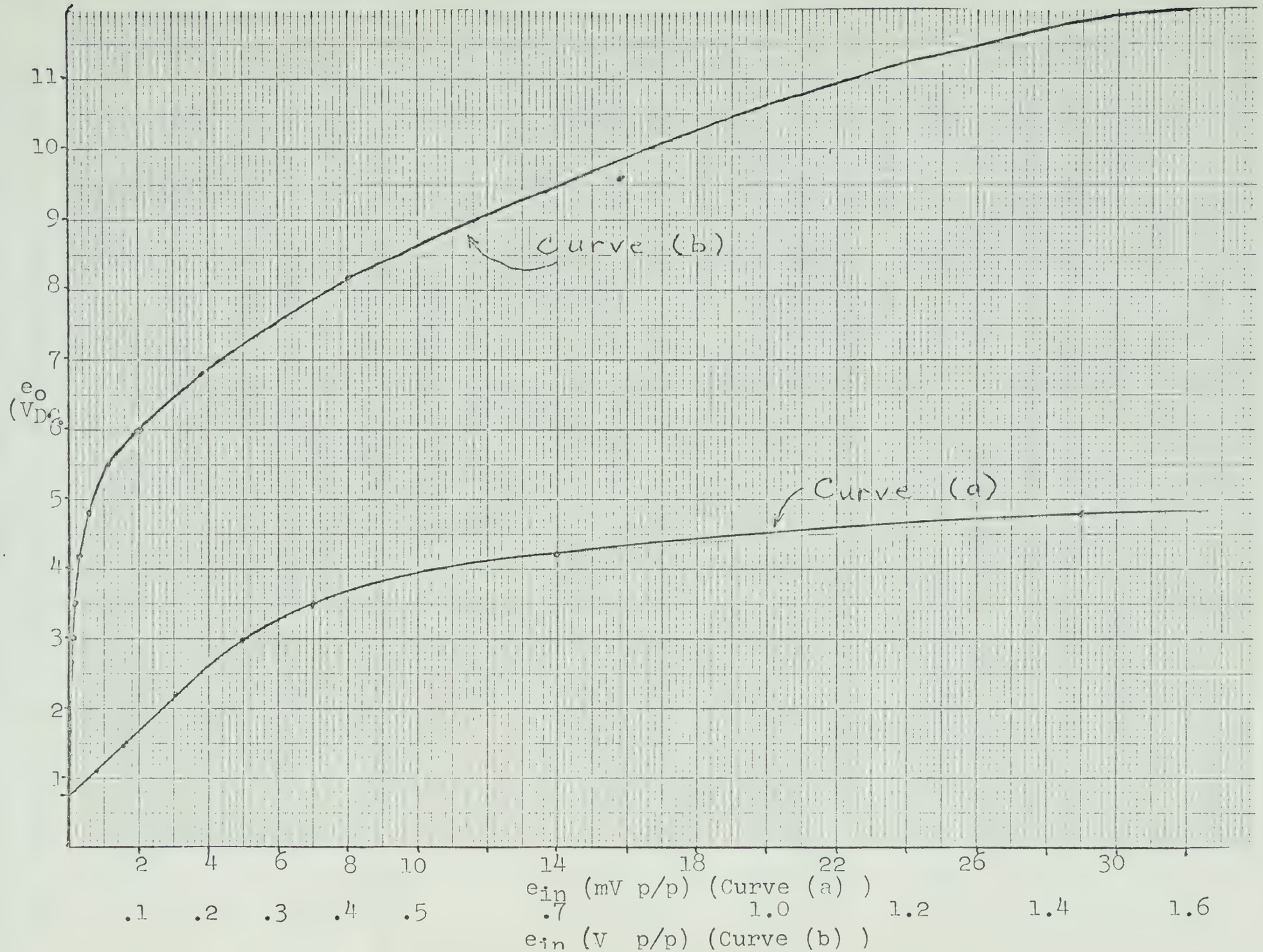
A_2 and A_2 perform the same function as A_2 and A_3 in figure 4.6. The offset voltage of A_2 is minimized by the bias network on the positive input. The signal e_1 is used in the motor sequence circuits (Section 4.8). A_3 incorporates two silicon diodes in the feedback loop to provide high gain when the output is less than 1 volt—at which point it decreases due to the diodes becoming forward biased. This provides an exanded region about the origin. C_f provides a small amount of filtering at 2 KHz (the second harmonic) without introducing an appreciable time delay. The bias network on the input reduces the effective deadzone of the servomotor.

The signal $e\phi$ is the input to the motor amplifier RT. It is a positive voltage which is first filtered (R_1,R_2,C_1), then subtracted from the main signal. This decreases the output voltage of A_3 (which is always positive) thereby slowing down motor RN until $e\phi$ has reduced to an appropriately small value. This ensures that RT achieves its proper value before RN. The germanium diode in the feedback loop prevents the output from going negative, which would cause motor RN to reverse direction.

Graph 7 is the measured transfer characteristic of the magnitude detector at 1 KHz (EMD. vs. ed). The maximum gain of the detector is about 1150 (Volts (D.C.)/volts (peak)) which occurs for ed < 4mV (p/p).



Graph 6 Experimental Magnitude Curves of A_1 (Figure 4.11)
for Three Input Levels



Graph 7 Transfer Characteristics of Magnitude Detector

4.7 MAGNITUDE DETECTOR POLARITY CIRCUITS

The output of the magnitude detector is a unipolar signal. A method of changing the polarity of this signal at the proper moments is required. As illustrated in Chapter 2 for the situation in which only RN is varying, the magnitude of ed is a minimum when it crosses the imaginary axis. Hence, the switching instants occur when $\phi = 90°$ and $\phi = 270°$. The circuits for the phase detector contain most of the signals which are required. Figure 4.12 contains the remainder of the circuitry.

The signal es(MD) is first buffered with an emitter follower (E.F.), then shifted in phase by 90° by two cascaded low pass filters to produce the signal referred to as -es(Q). This is applied to another E.F. and then applied to COMP 3. COMP 3, as for COMP 1 in figure 4.3, accurately represents the zero crossing on the rising part of the waveform. This output is buffered, then applied to the SET input of the FF. The output of G2 (ed*AGC) in figure 4.3 is applied to the clock input. There are two possibilities for $\overline{Q}$:

1) $\overline{Q}$ = 500 Hz square wave when ed lags es(Q)

2) $\overline{Q}$ = "0" when ed leads es(Q).

The monostable multivibrator, similar to the circuit in figure 4.5, results in:

1) $e_{POL(MD)} = 0$ when $\overline{Q}$ = square wave (ed lags es(Q))

2) $e_{POL(MD)} = 1$ when $\overline{Q} = 0$ (ed leads es(Q))

4.8 SEQUENCE OF MOTOR OPERATION

It was necessary to devise a sequence of operating the motors. This resulted from two causes:

1) When ϕ becomes zero for large values of ed, the angular error, though very small, becomes highly magnified as balance is approached (figure 4.13

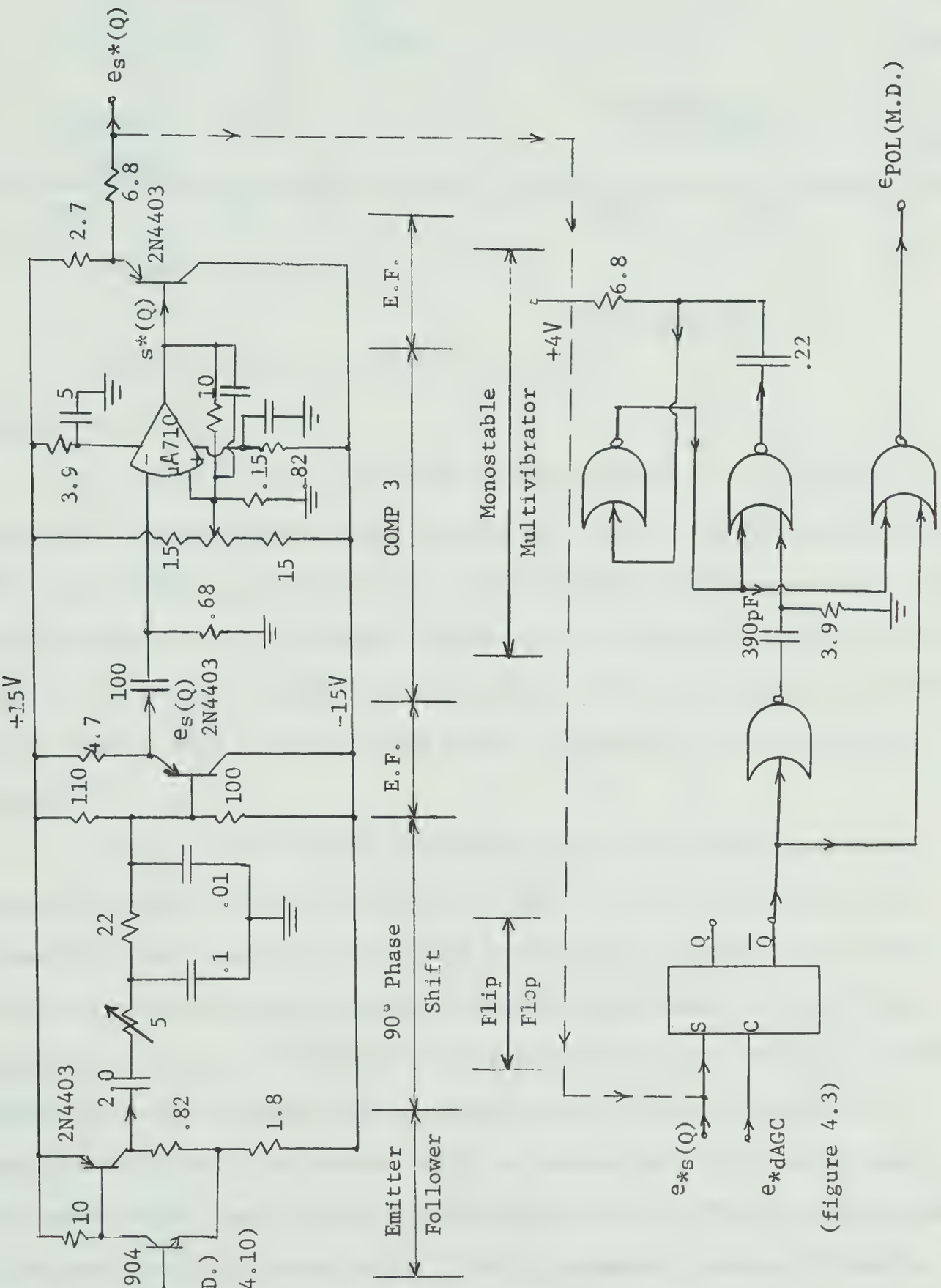


Figure 4.12 Magnitude Detector Polarity Circuits

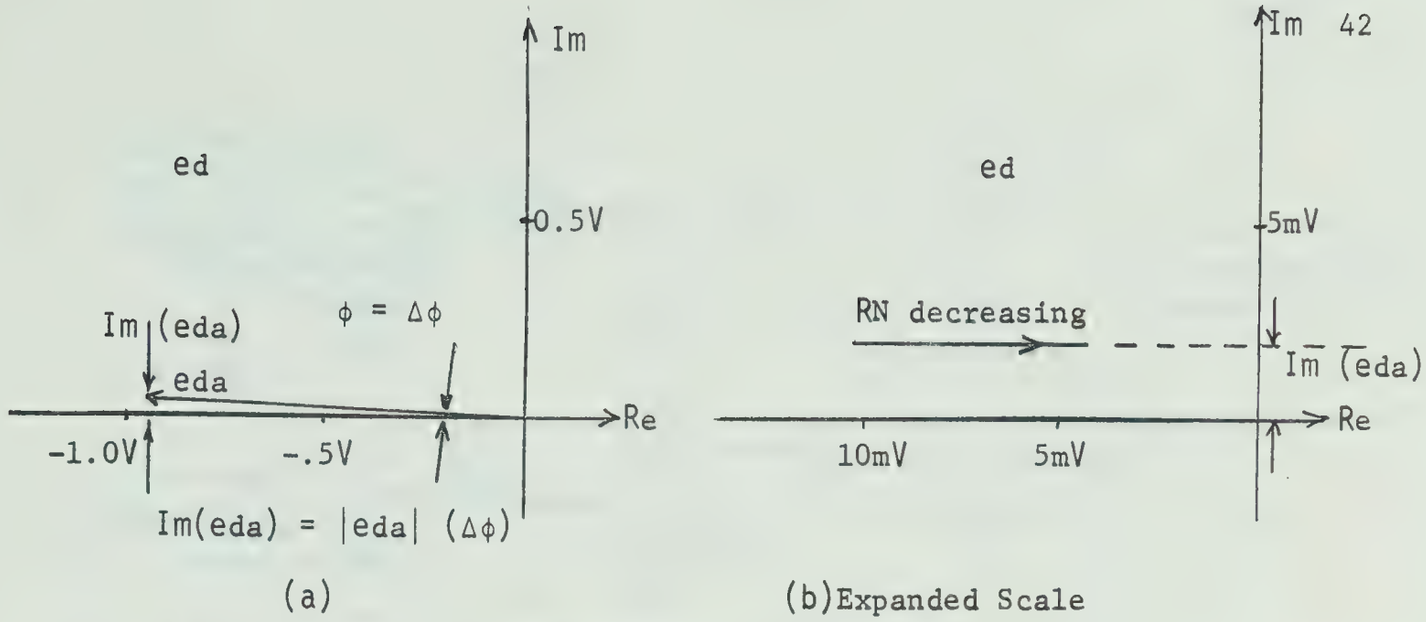


Fig. 4.13 Effect of Small Angular Error

if only RN is varied.

2) When ed is zero, the transfer characteristic of the phase detector turns into a relay characteristic because the locus of ed(RT) passing through the origin causes the phase angle to change abruptly from $+\phi_f$ to $-\phi_f$. (ϕ_f is a function only of the unknown capacitor and is directly related to the slope of the tangent of ed(RT) at the origin.) This situation can be shown to be unstable when there are three corner frequencies in the open loop system[8].

It was therefore decided to maintain the drive to the phase motor during the entire balancing procedure, except for the situation where ed became less than a certain small value ($\simeq$ 3mV p/p). At this value of ed, the gain in the phase angle feedback loop was high enough to cause large overshoots. It was also decided that if ed was less than 10mV (p/p) and the angular error was not less than a certain value, then the drive to the magnitude motor would be removed until the angular error did become small. This method would insure that the equilibrium value of RT would be achieved before the equilibrium value of RN. This is necessary because RT must be the equilibrium value when motor RT is turned off when ed $\lesssim$ 3mV.

The circuits in figure 4.14 accomplish the proper sequencing. G2 controls the input to motor RN, while Schmitt trigger 3 (S.T.3) controls

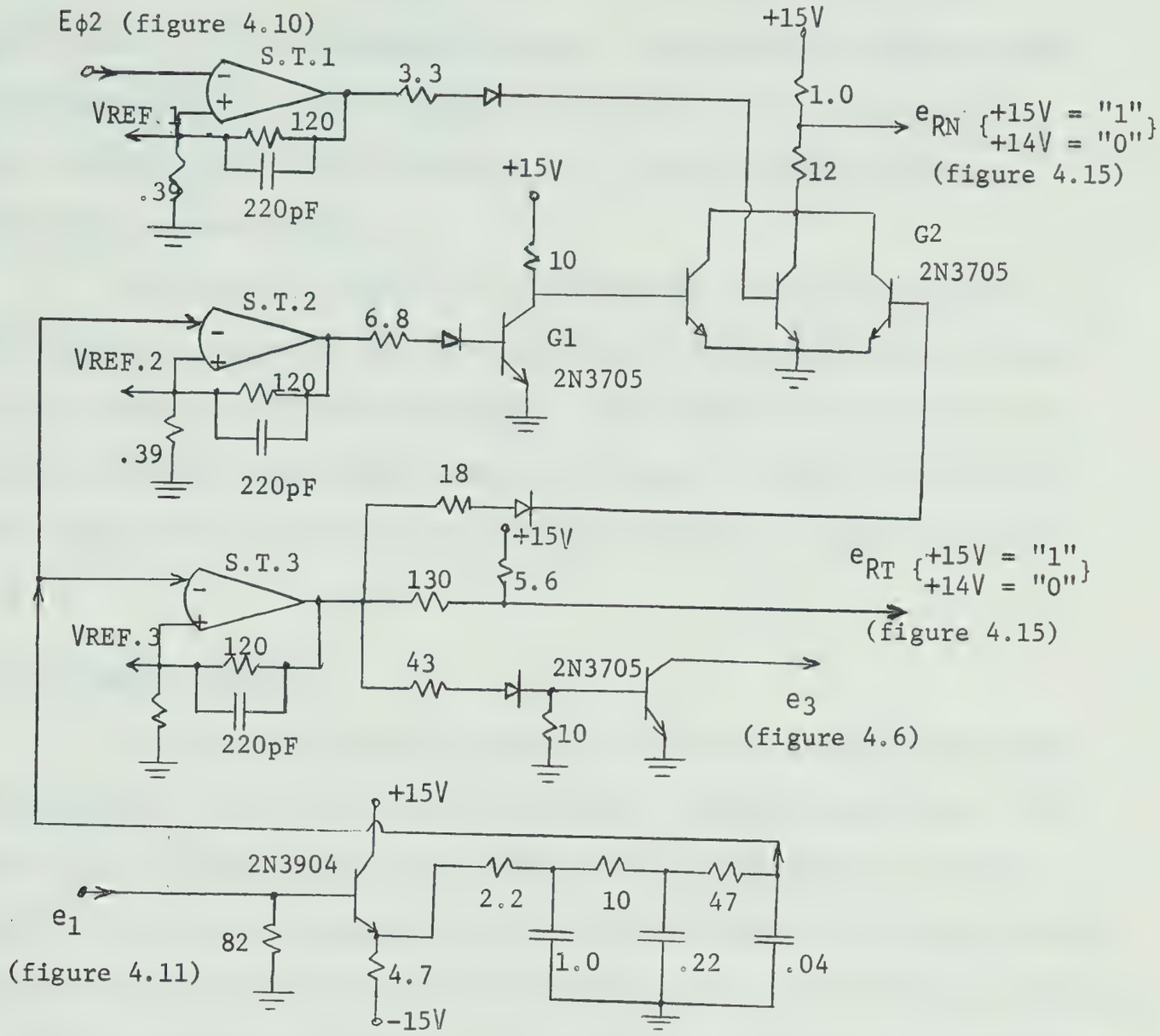


Figure 4.14 Motor Sequencing Circuits

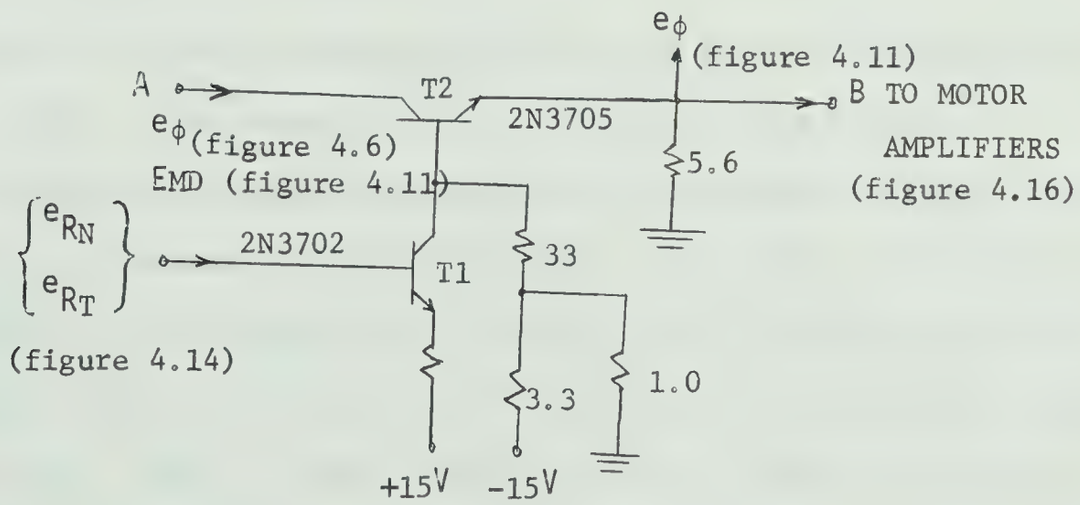


Figure 4.15 Motor Control Switch

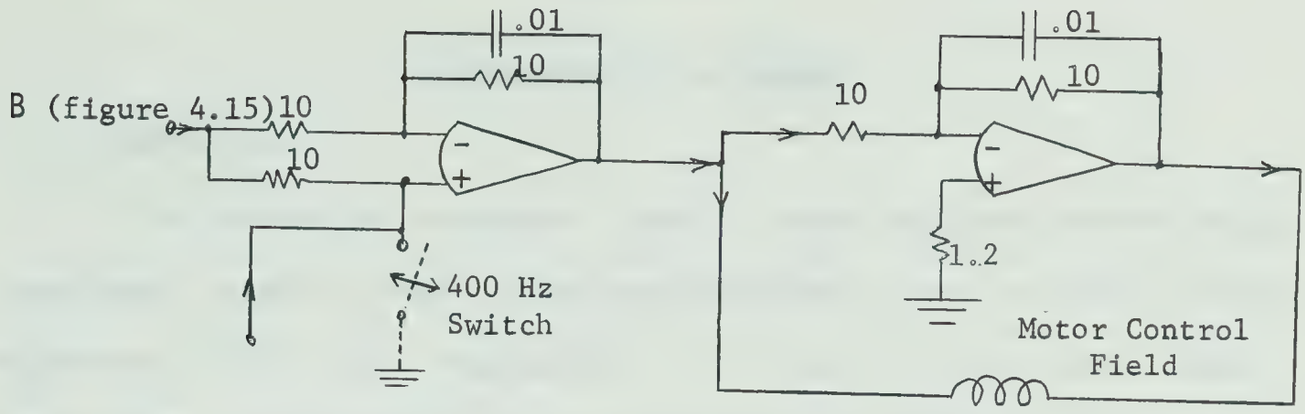
the input to motor RT. With e_{RN}, e_{RT} = "1", the motors are stopped; when e_{RN}, e_{RT} = "0", the motors are going. The reference voltages (VREF) are adjusted so that motor RT stops only when ed < 3mV, and motor RN stops only when 10mV > ed > 3mV and $\phi > 1°$. For all other conditions both motors are activated.

The outputs of figure 4.14, e_{RN} and e_{RT}, drive the switches controlling the inputs to the motor amplifiers. The same circuit (figure 4.15) is used for both motor amplifiers. With e_{RN}= +15V, Ti is off, T2 is reverse biased and no signal reaches the output. With e_{RN} = +14V, Ti is on, causing T2 to saturate and allowing the signal to pass freely from A to B.

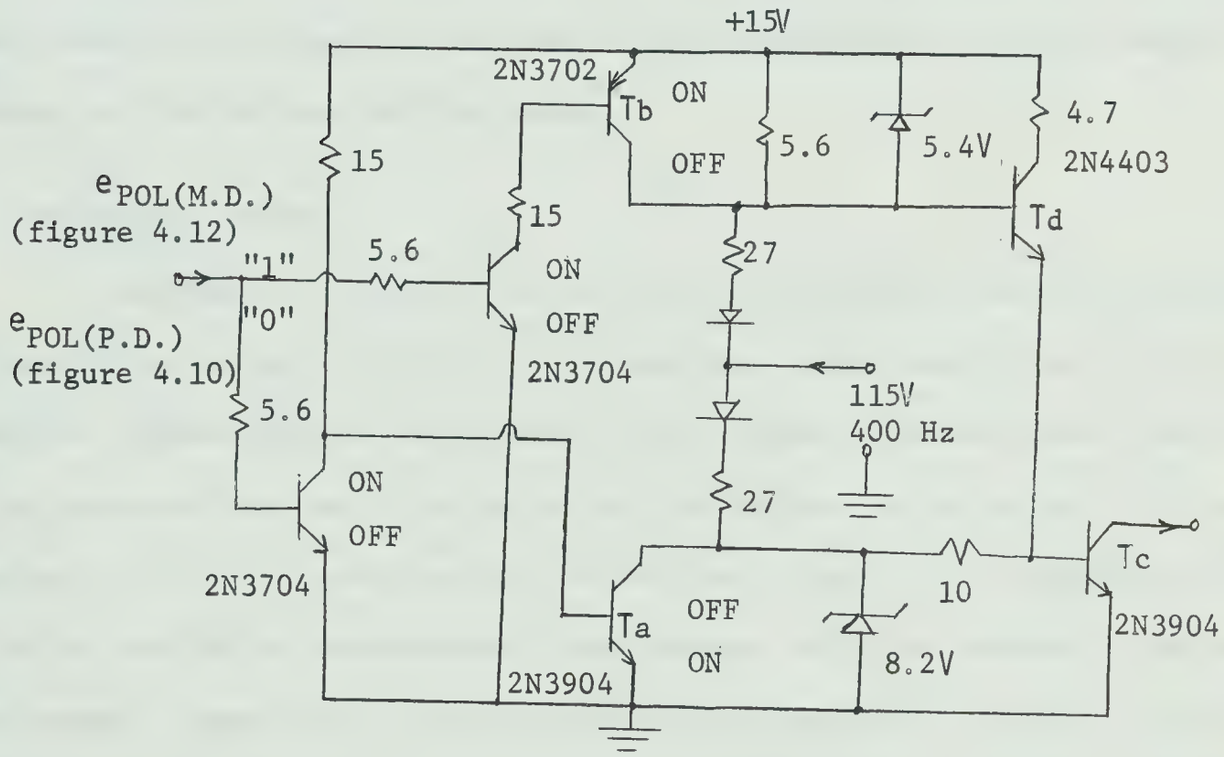
4.9 SERVOMOTOR CIRCUITS

The servomotors used to drive the variable resistors require two 400 Hz signals. One is a fixed signal having a constant amplitude. The other is the control signal whose amplitude is proportional to the drive signal. The control signal is shifted 90° with respect to the fixed signal. Two medium power amplifiers are used to supply the control field for each motor. The 400 Hz modulation is included in the design of the amplifiers. Figure 4.16 shows the circuits used.

The 400 Hz switch changes the gain of A_1 from +1 (switch open) to -1 (switch closed). The output is inverted by A_2 so that there is a differential signal of 60V (p/p) available for the control winding. The modulator uses an external 115V, 400 Hz supply. When e_{POL} = "0", Ta is on, Tb is off, and only the negative half cycles of the 115V supply turn Tc on (via Td). When e_{POL} = "1", Ta is off, Tb is on, and only the positive half cycles turn Tc on. Hence, as e_{POL} changes state, the modulation changes phase by 180°. This causes the signal on the control field to change phase by 180° which results in a reversal of torque on the motor.



(a) Amplifier Arrangement for Control Field



(b) Modulator

Figure 4.16 Motor Amplifiers and 400 Hz Modulator

The circuits for both motors (figure 4.16) are identical. The signals for the fixed fields are obtained from the same 400 Hz source which is applied to a phase shifter. The output of the phase shifter is applied directly to the fixed fields.

CHAPTER 5

PERFORMANCE OF INSTRUMENT

5.1 INTRODUCTION

The mechanical components (motors, rheostats, gear trains, supply transformer) used for this project are those which were available from the Department of Electrical Engineering at the time this study was started. They are not components designed specifically for this application. Therefore, the performance of this instrument at the present time is by no means the best which is obtainable. Specifically affected are the balancing time required, the absolute accuracy of the measurements, and the method of reading out the values for the unknown.

5.2 BALANCING PROCESS

When power is applied to the motors, RT quickly attains its equilibrium value, and moves very little for the remainder of the operation. RN, in the meantime, approaches its equilibrium value. When ed becomes less than 10mV, it is possible to observe the effect of the sequencing circuits. If the angular error is not small enough, RN will stop until RT is adjusted properly, at which time RN is reactivated. This process may occur several times in one measurement, depending on how accurately RT is adjusted. Perfect initial adjustment of RT should not require any repositioning as balance is approached.

The time to reach balance requires several seconds. If RN must change from its minimum to its maximum value, this time could be as long as 40 seconds. This is due to the fact that a very slow motor (motor RN) is used to drive a ten turn rheostat. This particular motor was used because it had a torque high enough to overcome the friction of the rheostat's wiper and consequently have a very small deadzone. The balancing time is not affected by RT since it can make one full turn in less than a second.

The resistances RT and RN are measured by a digital ohmmeter once automatic balance has been reached. The capacitance and dissipation are then calculated from equation 1.7. To determine the error of the automatic balance, the bridge detector output is observed on an oscilloscope with high sensitivity so that the rheostats may be adjusted manually to bring the output to zero. This then represents perfect balance, and the values of RT and RN are measured as before. The difference in RT and RN for these two measurements is the percentage error of the self balanced bridge. These errors are listed in Table 5.2, and show that the error in the capacitance is less than 0.1%, and the error in RT is generally less than 1 ohm.

5.3 EFFECTS OF NOISE AND STRAY CAPACITANCE

Noise on the bridge output (ed) causes the phase detector output to fluctuate about a nominal value. Should this value happen to be zero (corresponding to the condition where motor RN should be active when ed < 10mV), then these fluctuations may be large enough to activate the sequencing circuits, causing them to behave as though the angular error was not zero. This results in motor RN turning off when it should not be. Under these conditions, it takes longer for ed to traverse the region between 10mV and 3mV since the drive applied to motor RN is only sporadic, occurring when the fluctuations of the angular error pass through zero.

In an attempt to reduce the noise on the bridge, shielded leads are used to connect all the inputs and outputs of the bridge. This results in stray capacitance at the bridge terminals. Another source of stray capacitance occurs between the primary and secondary windings of the supply transformer, which is one intended for audio applications. These effects require that the equilibrium value of RT be negative for certain values of unknown. To compensate for this, a small resistor has been placed in series with the unknown.

This increases the effective dissipation factor of the unknown, which results in RT having a positive equilibrium value. A different value of series resistor (RS') is used for each range (Table 5.1).

The high gain of the phase detector when ed < 3mV causes RT to overshoot when a step input of phase angle is applied. If the equilibrium value of RT is zero (i.e. the wiper being at the junction of the beginning and the end of the rheostat), the overshoot will drive the wiper past the junction onto the other end of the rheostat. This causes RT to be driven continuously in one direction (a relaxation oscillation). To overcome this, RS' was made such that the minimum value of RT (≃ 7 ohms) is always large enough to prevent this. A rheostat with a space between the ends of the rheostat would overcome this problem.

Figure 5.1 is a detailed schematic diagram of the bridge. Included in it are the range and resistance measuring switches.

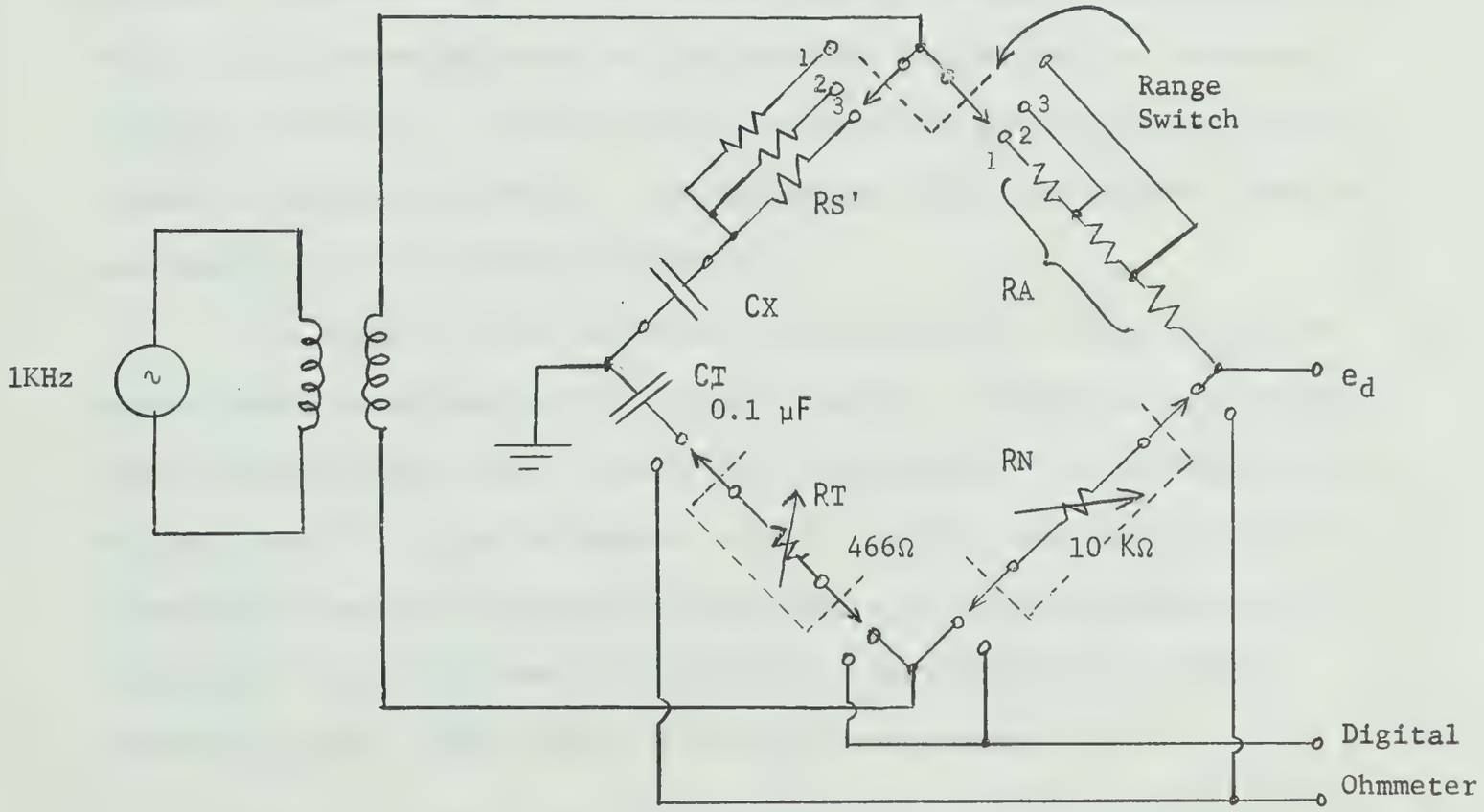


Figure 5.1 Wien Bridge Circuit



TABLE 5.1 RESISTANCE VALUES (RA,RS')

Range Switch Position	Value of RA	Value of RS'	Practical Range of Measurement
1	89.77 KΩ	220.5 Ω	.001 to .01 μf
2	8.977 KΩ	25.8 Ω	.01 to 0.1 μf
3	899.0 Ω	3.2 Ω	0.1 to 1.0 μf

Table 5.1 lists the values of the resistors for each range of measurement.

5.4 RESULTS

A sample of some typical measurements is shown in Table 5.2. RN (at balance) is the value of RN when the bridge has reached equilibrium. RN (ed = 0) is the value of RN when the bridge is manually balanced so that ed = 0. The percentage error of the automatic balance may be calculated from the difference. The components were also measured on the General Radio Impedance Bridge (Type 1650A). The percentage difference between these two measurements is also listed in Table 5.2.

The results listed in Table 5.2 show that the bridge is balanced automatically to within 0.1% of perfect balance. The error in the value of RT is generally less than 1.0 ohm. (This corresponds to a positional error of less than 0.8°.) The difference between the G.R. measurement and the calculated value of CS is generally less than 1%. No attempt was made to compare the measured values of D since the stray capacitance and the attempts to reduce their effect introduce large errors.

TABLE 5.2 RESULTS OF MEASUREMENTS

All resistance are in ohms. All capacitances are in μF.

CX	RN (at Balance)	RN (ed=0)	Error RN	RT (at Balance)	RT (ed=0)	Error RT	Value of CS	% Error with G.R.
1.0	8963 8965	8967 8960	4 5	14.2 13.7	15.2 15.2	1.0 1.5	.996	-0.9%
.68	6327 6322	6326 6318	1 4	9.0 8.0	8.0 9.0	1.0 1.0	.704	-0.6%
.25	2366 2364	2365 2364	1 0	9.0 9.0	9.0 9.0	0 0	.2365	-0.7%
.10	891.2 890.7	891.2 890.7	0 0	8.5 8.5	8.5 8.5	0 0.5	.0994	-0.8%
.10	891.2 890.6	891.0 890.4	.2 .2	8.5 8.5	8.5 8.0	0 0.5	.0994	-0.8%
.068	5942 5933	5941 5937	1 4	4.4 4.0	4.6 4.9	0.2 0.9	.0662	-0.8%
.05	4025 4020	4024 4023	1 3	8.0 8.0	8.0 8.0	0 0	.0448	-1.1%
.03	2739 2737	2738 2736	1 1	13.5 13.1	13.2 13.1	0 0	.03053	-0.7%
.02	1844 1843	1844 1841	0 2	17.3 15.7	16.2 16.2	1.1 0.5	.02056	-0.7%
.01	892.5 892.0	892.1 891.9	.4 .1	10.1 10.6	10.1 10.1	0 0.5	.0094	-0.8%
.01	8916 8925	8929 8931	13 7	11.1 11.1	10.1 10.1	1.0 1.0	.00995	-0.7%
.008	7215 7203	7211 7210	4 7	7.5 10.0	8.0 8.5	0.5 1.5	.00803	-1.5%
.005	4563 4553	4560 4556	3 3	11.7 12.1	11.6 11.6	0.1 0.5	.00508	-2.0%
.003	2620 2617	2625 2618	5 1	18.4 19.3	17.9 18.8	0.5 0.5	.002923	-2.3%
.001	860.1	858.6	1.5	46.0	31.2	14.8	.000967	-3.3%

5.5 CONCLUSIONS

This project has shown that automatically balancing a capacitance bridge using positional devices is feasible.

The balance achieved by the instrument is quite accurate. The balancing error of 0.1% (using the criterion that perfect balance is 0.0%) is comparable to that of commercially available impedance measuring instruments. While it is acknowledged that there are other larger sources of error (stray capacitance, imperfect reference components), these could be reduced by taking the same precautions in the bridge circuit as is done in the commercial instruments. The corresponding error in the dissipation factor is generally less than one ohm. This represents a large percentage error when the equilibrium value of RT is small (< 7ohms); however, it is a very small error when shaft position is considered (< 0.8°).

Three main areas of improvement to make the bridge practical are in the speed of measurement, the absolute accuracy, and the readout of the parameters. A faster servomotor and a single turn rheostat for RN would considerably reduce measuring time. Improving the accuracy would involve taking greater care in the construction of the bridge itself. The readout could be accomplished using a photo-electrical shaft encoder to present a digital measurement of shaft position and hence resistance. This method can be made very accurate, and would not contribute to the deadzone or the inertia of the system.

LIST OF REFERENCES

1. Applications Engineering Section of Burr Brown Research Corporation: *Handbook of Operational Amplifier Applications;* Burr Brown Research Corporation, Tucson, Arizona; 1963.
2. Applications Engineering Section of Burr Brown Research Corporation: *Handbook of Operational Amlifier Active RC Networks;* Burr Brown Research Corporation, Tucson, Arizona; 1966.
3. Engineering Staff of Texas Instruments, Inc.: *Transistor Circuit Design;* McGraw Hill Book Company, Inc., New York; 1963.
4. Fitchen, F. C.: *Transistor Circuit Analysis and Design;* D. Van Nostrand Co.; 1960.
5. Frank, E.: *Electrical Measurement Analysis;* McGraw Hill Book Company, Inc., New York; 1959.
6. Fulks, R. G.: The Automatic Capacitance Bridge; *The General Radio Experimenter,* Vol.39, No. 4, April 1965; General Radio Company, West Concord, Mass.; 1965.
7. General Radio Company: *Operating Instructions, Type 1650-A Impedance Bridge;* General Radio Company, West Concord, Mass.; 1961.
8. Gibson, J. E.: *Non-Linear Automatic Control;* McGraw Hill Book Company, Inc., New York; 1963.
9. Hague, B.: *Alternating Current Bridge Method;* Sir Isaac Pitman and Sons, Ltd., London; 1938.
10. Joyce, M. V., and K. K. Clarke: *Transistor Circuit Analysis;* Addison-Wesley Publishing Company, Inc.; 1961.
11. Kuo, B. C.: *Automatic Control Systems;* Prentice Hall, Inc., New York; 1962.
12. Stout, M. B.: *Basic Electrical Measurements;* Prentice Hall, Inc., New York; 1950.

APPENDIX I

APPENDIX I

LOCUS OF A CIRCLE

The function f (x) (equation 1.1) may be shown to be a circle.

$$f(x) = \frac{a + jbx}{c + j\,x} \qquad \text{(A 1.1)}$$

$$= b + \frac{a - bc}{c + jx} \qquad \text{(A 1.2)}$$

where a, b, c are complex constants
x is the variable.

Consider equation A 1.2. It consists of a constant vector (b) and a variable vector. The locus of f (x) in the complex plane is determined by the variable vector. Denoting the variable vector as W (x) and introducing new complex constants yields:

$$W(x) = \frac{A}{B+jX} \qquad \text{(A 1.3)}$$

$$= \frac{A_1 + j\,A_2}{B_1 + j\,(B_2 + X)} \qquad \text{(A 1.4)}$$

where $A = A_1 + j\,A_2$

$B = B_1 + j\,B_2$

To demonstrate that equation A 1.3 is a circle, (and hence A 1.1 also) equation A 1.4 will be rationalized.

$$W(x) = \frac{A_1B_1+A_2(B_2+X) + j\,\{A_2B_1-A_1(B_2+X)\}}{B_1^2 + (B_2+x)^2} \qquad \text{(A 1.5)}$$

This may be separated into a real and an imaginary part.

$$W(x) = u + j\,V \qquad \text{(A 1.6)}$$

$$u = \frac{A_1B_1+A_2(B_2+X)}{D} \qquad \text{(A 1.7)}$$

$$V = \frac{A_2B_1-A_1(B_2+X)}{D} \qquad \text{(A 1.8)}$$

where $D = B_1^2 + (B_2+X)^2$

Squaring equations A 1.7 and A 1.8, and adding the results yields:

$$u^2 + v^2 = \frac{A_1^2 + A_2^2}{D} \qquad \text{(A 1.9)}$$

Multiplying equations A 1.7 and A 1.8 by A_1 and A_2 respectively, and adding, results in equation A 1.10.

$$A_1u+A_2V = \frac{A_1^2 + A_2^2 B_1}{D} \qquad \text{(A 1.10)}$$

Now equations A 1.9 and A 1.10 may be combined.

$$u^2+V^2 = \frac{A_1}{B_1} u + \frac{A_2}{B_1} V \qquad \text{(A 1.11)}$$

Rearranging the terms, and completing the squares results in equation A 1.12.

$$(u - \frac{A_1}{2B_1})^2 + (V - \frac{A_2}{2B_1})^2 = \frac{A_1^2 + A_2^2}{(2B_1)^2} \qquad \text{(A 1.12)}$$

This is the equation of a circle with a center and radius as indicated below:

$$\text{Radius} = \frac{(A_1^2 + A_2^2)^{1/2}}{2B_1} = \frac{|A|}{2B_1} \qquad \text{(A 1.13)}$$

Center {uc,Vc}:

$$uc = \frac{A_1}{2B_1} \qquad \text{(A 1.14)}$$

$$Vc = \frac{A_2}{2B_1} \qquad \text{(A 1.15)}$$

In terms of the constants of equation A 1.1, these become:

$$\text{Radius} = \frac{|a - bc|}{2 \text{ Re } \{c\}} \qquad \text{(A 1.16)}$$

$$uc = \frac{\text{Re } \{a - bc\}}{2 \text{ Re } \{c\}} + \text{Re } \{b\} \qquad \text{(A 1.17)}$$

$$Vc = \frac{\text{Im } \{a - bc\}}{2 \text{ Re } \{c\}} + \text{Im } \{b\} \qquad \text{(A 1.18)}$$

APPENDIX II

APPENDIX II

SPECIFICATIONS OF μA 709

GENERAL DESCRIPTIONS - The μA709 is a high-gain operational amplifier constructed on a single silicon chip using the Fairchild Planar epitaxial process. It features low offset, high input impedance, large input common mode range, high output swing under load and low power consumption. The device displays exceptional temperature stability and will operate over a wide range of supply voltages with little degradation of performance. The amplifier is intended for use in DC servo systems, high impedance analog computers, in low-level instrumentation applications and for the generation of special linear and nonlinear transfer functions.

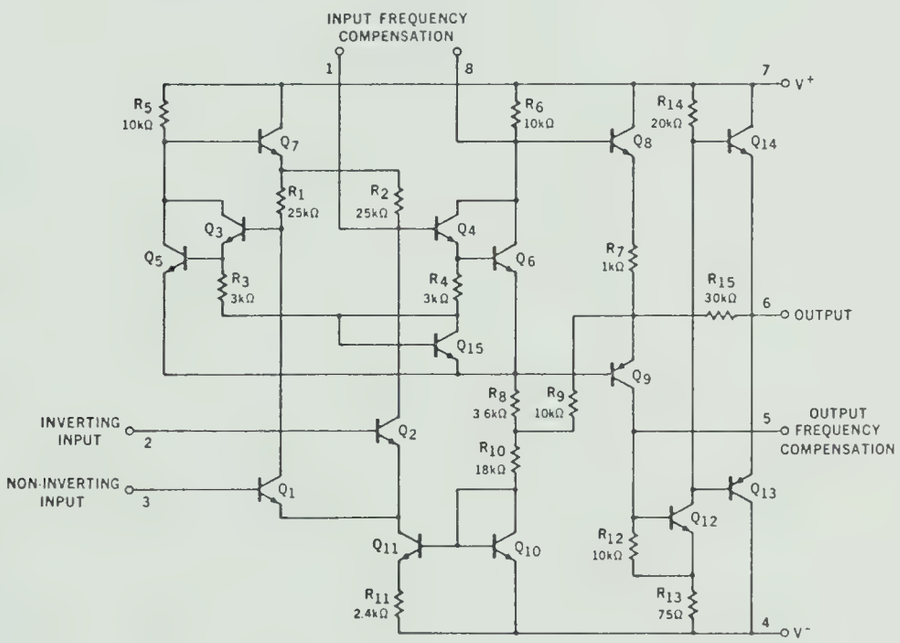


Figure A 2.1 Schematic Diagram of μA 709

ELECTRICAL CHARACTERISTICS

$\pm 9V \leq V_S \leq \pm 15V$

$T_A = 25°C$

Parameter (see definitions)	Conditions	Min.	Typ.	Max.	Units
Input Offset Voltage	$R_S \leq 10 k\Omega$		1.0	5.0	mV
Input Offset Current			50	200	nA
Input Bias Current			200	500	nA
Input Resistance		150	400		k Ω
Output Resistance			150		Ω
Power Consumption	$V_S = \pm 15$ V		80	165	mW
Transient Response	$V_{in} = 20$ mV, $R_L = 2$ kΩ,				
Risetime	$C_1 = 5000$ pF, $R_1 = 1.5$ kΩ, $C_2 = 200$ pF, $R_2 = 50$ Ω		0.3	1.0	μs
Overshoot	$C_L \leq 100$ pF		10	30	%
The following specifications apply for $-55°C \leq T_A \leq +125°C$:					
Input Offset Voltage	$R_S \leq 10$ kΩ			6.0	mV
Average Temperature Coefficient of Input Offset Voltage	$R_S = 50$ Ω		3.0		μV/°C
	$R_S \leq 10$ kΩ		6.0		μV/°C
Large-Signal Voltage Gain	$V_S = \pm 15$ V, $R_L \geq 2$ kΩ, $V_{out} = \pm 10$ V	25,000	45,000	70,000	
Output Voltage Swing	$V_S = \pm 15$ V, $R_L \geq 10$ kΩ	±12	±14		V
	$V_S = \pm 15$ V, $R_L \geq 2$ kΩ	±10	±13		V
Input Voltage Range	$V_S = \pm 15$ V	±8.0	±10		V
Common Mode Rejection Ratio	$R_S \leq 10$ kΩ	70	90		dB
Supply Voltage Rejection Ratio	$R_S \leq 10$ kΩ		25	150	μV/V
Input Offset Current	$T_A = +125°C$		20	200	nA
	$T_A = -55°C$		100	500	nA
Input Bias Current	$T_A = -55°C$		0.5	1.5	μA
Input Resistance		40	100		k Ω

APPENDIX III

APPENDIX III

SPECIFICATIONS OF μA 710

GENERAL DESCRIPTION — The μA710 is a differential voltage comparator intended for applications requiring high accuracy and fast response times. It is constructed on a single silicon chip using the Fairchild Planar epitaxial process. The device is useful as a variable threshold Schmitt trigger, a pulse height discriminator, a voltage comparator in high-speed A-D converters, a memory sense amplifier or a high-noise immunity line receiver. The output of the comparator is compatible with all integrated logic forms.

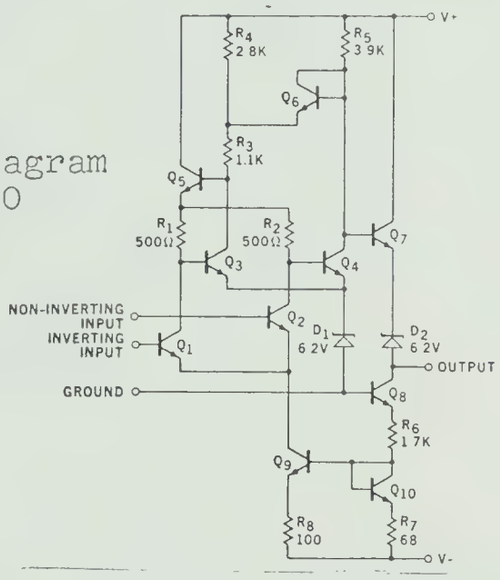


Figure A 3.1 Schematic Diagram of uA 710

ELECTRICAL CHARACTERISTICS:

$V^+=12V$ $V^-=-6V$
$T_A=25^\circ C$

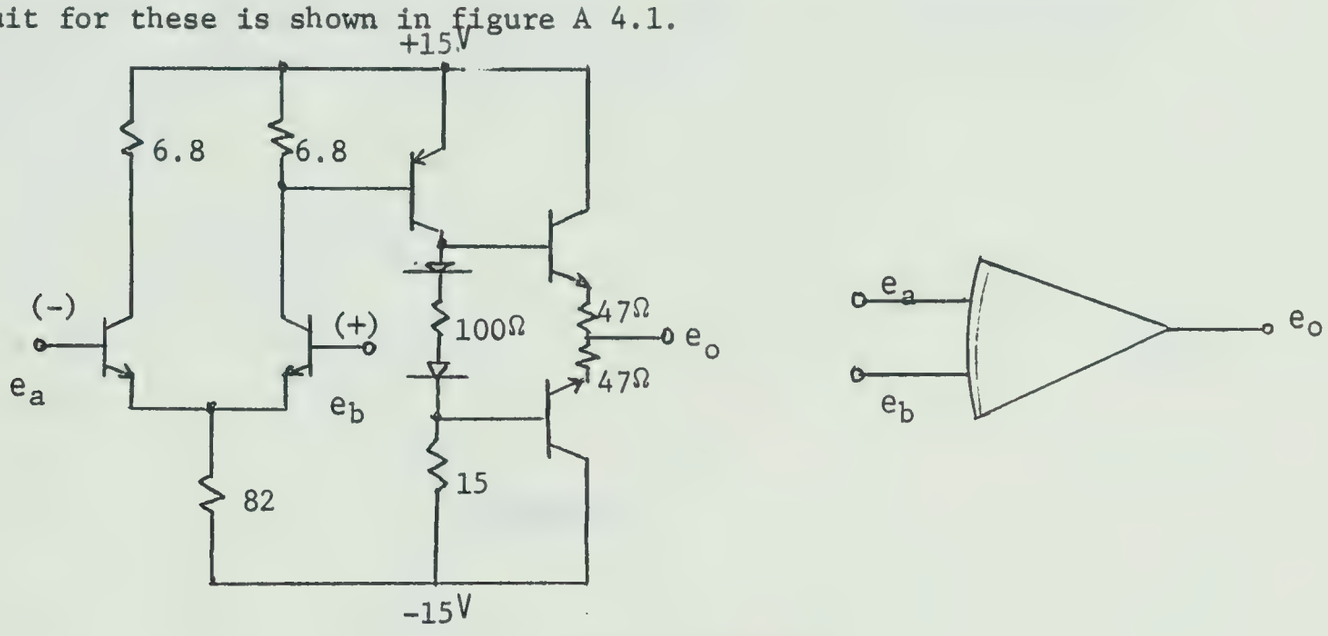
Parameter (see definitions)	Conditions	Min.	Typ.	Max.	Units
Input Offset Voltage	V_{out} = +1.4 V, $R_S \leq 200\,\Omega$		2.0	5.0	mV
Input Offset Current	V_{out} = +1.4 V		1.0	10.0	μA
Input Bias Current			25	75	μA
Voltage Gain		750	1500		
Output Resistance			200		Ω
Response Time (Note 3)			40		nsec
Input Voltage Range	V^- = -7.0 V	±5.0			V
Differential Input Voltage Range		±5.0			V
Positive Output Level	$V_{in} \geq 15$ mV, $0 \leq I_o \leq 0.5$ mA	+2.5	+3.2	+4.0	V
Negative Output Level	$V_{in} \geq 15$ mV	-1.0	-0.5	0	V
Output Sink Current	$V_{in} \geq 15$ mV, $V_{out} \geq 0$	1.6	2.5		mA
Positive Supply Current	$V_{out} \leq 0$		6.4		mA
Negative Supply Current			5.5		mA
Power Consumption					
TO-5 Package			110	175	mW
Flat Package			110	150	mW
The following specifications apply for $-55^\circ C \leq T_A \leq +125^\circ C$:					
Input Offset Voltage (Note 4)	$R_S \leq 200\,\Omega$			6.0	mV
Input Offset Current (Note 4)				20	μA
Input Bias Current				150	μA
Temperature Coefficient of Input Offset Voltage (Note 4)			5.0		μV/°C
Voltage Gain		500			

APPENDIX IV

APPENDIX IV

DISCRETE COMPONENT OPERATIONAL AMPLIFIER

A majority of the circuits used in the instrument makes use of operational amplifiers of the discrete component type. The typical circuit for these is shown in figure A 4.1.



A 4.1 Typical Operational Amplifier

The Schmitt triggers use the same circuit except they do not require the push-pull emitter follower output stage.



APPENDIX V

APPENDIX V

EFFECT OF STRAY CAPACITANCES

It may be shown that stray capacitance across the resistors RA and RN could result in the bridge being unable to balance itself if the dissipation of the unknown is very small. Consider the bridge equation (equation 1.5) with the stray capacitances in parallel with RA and RN (CA and CN).

$$\frac{ed}{es} = \frac{RNZS - RAZT}{(RA + RN)(ZT + ZS)} \qquad (A\ 5.1)$$

$$RN \rightarrow \frac{RN}{1 + STN} \qquad (A\ 5.2)$$

$$RA \rightarrow \frac{RA}{1 + STA} \qquad (A\ 5.3)$$

$$ZS = \frac{1 + STS}{SCS} \qquad (A\ 5.4)$$

$$ZT = \frac{1 + STT}{SCT} \qquad (A\ 5.5)$$

After substituting these into A 5.1, the bridge equation becomes:

$$\frac{ed}{es} = \frac{\frac{RN}{1+STN} \cdot \frac{1+STS}{SCS} - \frac{RA}{1+STA} \cdot \frac{1+STT}{SCT}}{(\frac{RN}{1+STN} + \frac{RA}{1+STA})(\frac{1+STS}{SCC} + \frac{1+STT}{SCT})} \qquad (A\ 5.6)$$

Since only the conditions at balance are of interest, the numerator may be set equal to zero.

$$\frac{RN}{1+STN} \cdot \frac{1+STS}{SCS} = \frac{RA}{1+STA} \cdot \frac{1+STT}{SCT} \qquad (A\ 5.7)$$

This may be simplified to:

$$(1-KRKC) + S(TT-TN-(TA+TS)KRKC) - S^2(TTTN-TATSKRKC) = 0 \qquad (A\ 5.8)$$

where: $KR = \frac{RN}{RA}$

$KC = \frac{CT}{CS}$

One of the conditions for equation A 5.8 to be true is:

$$TT+TN - (TA+TS)KRKC = 0 \qquad \text{(A 5.9)}$$

From this, the equilibrium value of TT (and hence RT) is obtained.

$$TT = (TA+TS)KRKC - TN \qquad \text{(A 5.10)}$$

Examination of equation A 5.10 shows that if the dissipation factor of the unknown is small enough ($TS \rightarrow 0$) and the stray capacitance across RN is large enough ($TN \rightarrow$ large) then TT (and hence RT) must be negative for balance. This effect may be counteracted by deliberately making either TS or TA larger. This, however, makes subsequent measurements less meaningful. If the effect is small, the only noticeable error will be in the indicated value of TS (and hence D).

APPENDIX VI

APPENDIX VI

MECHANICAL COMPONENTS

The mechanical position of the capacitance bridge uses two servomotors, each coupled to a variable resistor by a gear train.

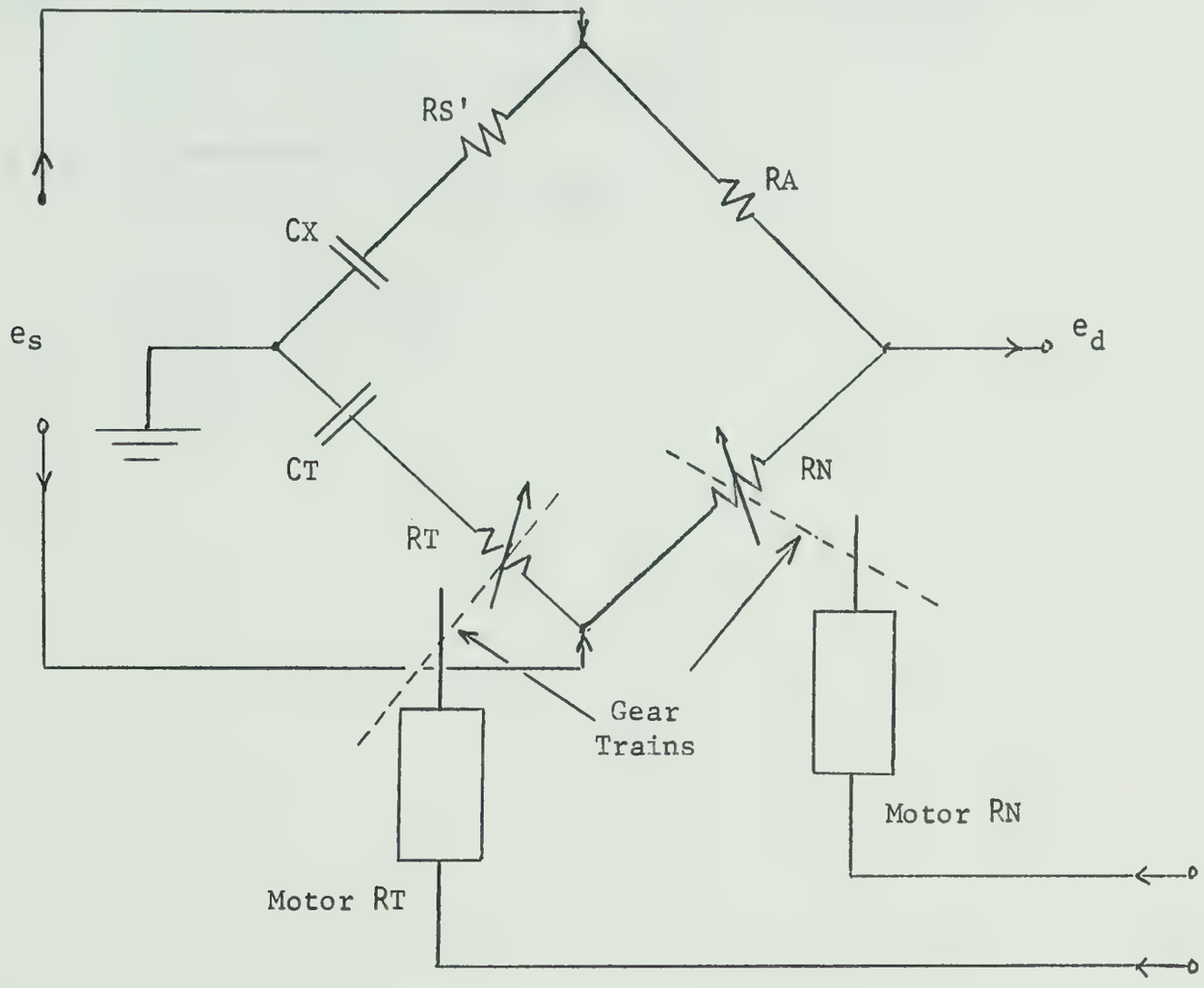


Figure A 6.1 Diagram of Mechanical Bridge Components

RT: Voak Engineering, Model CR1
Total resistance 466 ohms
Single turn (continuous)
Linearity $< \pm 0.1\%$

RN: Gibbs Micropot Potentiometer, Type N, Serial 61037
Total resistance 10,000 ohms
Ten turn, wirewound
Linearity $< \pm 0.05\%$



Motor RT: Kearfott Company Inc., Motor Generator Type R800-1A
Two phase, 400 Hz
115V RMS - Control and fixed fields
No load speed 4500 RPM
Stalled Torque 1.45 ounce-inches

Motor RN: Thomas A. Edison Industries, Geared Motor Generator
Two phase, 400 Hz
30V RMS - Control and fixed fields
No load speed 63 RPM
Stalled torque 38 ounce-inches

CT: Southern Electronics
0.1 μF ± 0.5%, 200V
Polystyrene

B29900